IAEA
International Atomic Energy Agency

INDC(NDS)-0560
Distr. HCP

INDC International Nuclear Data Committee

Summary Report

Second Research Coordination Meeting on Heavy Charged-Particle Interaction Data for Radiotherapy

National Institute of Nuclear Physics, Catania, Italy
8-12 June 2009

Prepared by

Hugo Palmans
National Physical Laboratory
United Kingdom

and

Roberto Capote Noy
IAEA Nuclear Data Section
Vienna, Austria

May 2010

Selected INDC documents may be downloaded in electronic form from
http://www-nds.iaea.org/reports-new/indc-reports/
or sent as an e-mail attachment.
Requests for hardcopy or e-mail transmittal should be directed to *services@iaeand.iaea.org*
or to:
Nuclear Data Section
International Atomic Energy Agency
Vienna International Centre
PO Box 100
A-1400 Vienna
Austria

Printed by the IAEA in Austria

May 2010

INDC(NDS)-0560
Distr. HCP

Summary Report

Second Research Coordination Meeting on Heavy Charged-Particle Interaction Data for Radiotherapy

National Institute of Nuclear Physics, Catania, Italy
8-12 June 2009

Prepared by

Hugo Palmans
National Physical Laboratory
United Kingdom

and

Roberto Capote Noy
IAEA Nuclear Data Section
Vienna, Austria

Abstract

A summary is given of the 2nd Research Coordination Meeting (RCM) on *Heavy Charged-Particle Interaction Data for Radiotherapy*. The programme to compile and evaluate charged-particle nuclear data for therapeutic applications was reviewed. Technical discussions and the resulting work plan of the Coordinated Research Programme are summarized, along with planned actions and deadlines. Participants' reports at the 2nd RCM are also included in this report.

May 2010

TABLE OF CONTENTS

1. Introduction

A Consultants' Meeting (CM) was organised at the IAEA in Vienna in November 2006 to identify the needs for comprehensive evaluated data for nuclear interaction cross sections, including recommendations on types of nuclear data and their accuracy[1]. One further aim was to cover all steps of proton and heavier ion therapy delivery by putting discussions between experts in the field of proton and ion therapy, proton and ion dosimetry and proton and ion Monte Carlo simulations high on the agenda. Main requirements were identified and the following recommendations were agreed:

- Initiate a programme of work focused on nuclear data evaluations for charged-particle therapeutic applications.
- Invite representatives of Monte Carlo code development teams to take part in the programme.

To meet these requirements, the Coordinated Research Project (CRP) named "Heavy charged-particle interaction data for radiotherapy" (CHARPAR) started in 2007 with the 1st Research Coordination Meeting (RCM) held at IAEA Headquarters, Vienna, from 6 to 9 November 2007, and attended by eleven CRP participants and one external observer. A truly co-ordinated programme of work was agreed among the participants, leading to several additional actions to be undertaken. Technical discussions and the resulting work plan of the Coordinated Research Programme were summarized in IAEA Report **INDC (NDS)-0523**[2].

The 2nd RCM of the CHARPAR CRP was hosted by the INFN Laboratori Nazionali del Sud, Catania (Italy) from 8-12 June 2009, and attended by eleven CRP participants. The local organizer of the meeting was G. Cuttone. The IAEA was represented by R. Capote, who served as Scientific Secretary. H. Paganetti (Massachusetts General Hospital, Boston, USA) was elected Chairman of the meeting and H. Palmans from National Physical Laboratory, United Kingdom, agreed to act as rapporteur. The adopted Agenda is attached (Appendix 1) as well as the list of participants and their affiliations (Appendix 2).

The participants reviewed the status of the work within the CRP and discussed scientific and technical details. In particular, issues related to sensitivity studies, neutron production in charged-particle therapy and relevant benchmarks for data validation were debated in detail. Section 2 summarizes the work done by participants. Primary aims of this meeting were to coordinate related tasks, and to assess assigned responsibilities and deadlines. The research objectives and expected outputs of the CRP remain those agreed during the 1st RCM (see **INDC(NDS)-0523**). The following outcomes are expected:

- Make available experimental and recommended nuclear data parameterisations on the web, recommending new experiments when needed.
- Make available recommended hadronic physics settings for the considered Monte Carlo codes and applications on the web.
- Publication of a comprehensive technical document.

The draft version of the technical document is expected to be discussed at the third and final RCM of the project in 2010.

---

[1] R. Capote and S. Vatnisky, *Summary Report of Consultants' Meeting on "Nuclear Data of Charged-Particle Interactions for Medical Therapy Applications"*, **INDC(NDS)-0504** (IAEA, Vienna, January 2007).

[2] H. Palmans and R. Capote, *Summary Report of first Research Coordination Meeting on "Heavy Charged-Particle Interaction Data for radiotherapy"*, **INDC(NDS)-0523** (IAEA, Vienna, April 2008).

The actions to be undertaken prior to the next RCM to be held in late 2010 were agreed, together with their relative time-schedule and deadlines (if not explicitly stated otherwise, default deadline for all actions is the next RCM). The status of the work, the assigned actions and deadlines and the recommendations to best coordinate efforts are summarized below.

2. Progress Reports

2.1. H. Paganetti (MGH and Harvard University)

New aspect compared to last year's meeting: Prompt gamma range detection. Goal of these efforts is to assess the feasibility of detecting gamma-rays emitted during proton inelastic scattering as a method for identifying the distal edge of the proton depth-dose profile. The most pressing technical question to address is the determining of the sensitivity and spatial resolution that can be practically attained in a clinical setting. MGH has done some Monte Carlo work on this issue.

A. Cross sections
List of treatment head materials is needed. The importance of double-differential cross sections may depend on whether these materials are used in either beam shaping or beam modifying devices and on what their typical position in the treatment head is. The sensitivity of physics data depends on the application.

- The materials used in most treatment heads are:
  - Steel (beam scatterers, collimator housing, magnet housing, detector housing)
  - Lexan (beam scatterers, modulators, compensators)
  - Lead (beam scatterers, modulators)
  - Aluminum (beam scatterers, modulators, collimator housing, ion chambers)
  - Carbon (modulators): There can be a few different carbon types (with different densities).
  - Brass (collimators, apertures, scanning magnets)
  - Nickel (collimators)
  - Copper (scanning magnets)
  - PVC (ion chambers)
  - Mylar (ion chambers)

Material compositions are

Brass	Cu 0.7, Zn 0.3
Lexan	H 0.055491, C 0.755751, O 0.188758
Mylar	H 0.041959, C 0.625017, O 0.333025
PVC	H 0.048380, C 0.384360, Cl 0.567260
Steel	C 0.0015, Si 0.01, P 0.00045, S 0.0003, Cr 0.19, Mn 0.02, Fe 0.67775, Ni 0.1

- Contribution of nuclear interactions (i.e. cross section data) from human tissue materials to dose when doing Monte Carlo dose calculation in patient geometries.

The materials in the patient are tantalum and gold for metallic implants and tissue materials as listed in Table 1 below [1].

Table 1: Tissue composition and corresponding density range given in Honsfield units (HU) as used at MGH [1].

HU range	H	C	N	O	Na	Mg	P	S	Cl	Ar	K	Ca
[; -951]			75.5	23.2						1.3		
[-950 ; -121]	10.3	10.5	3.1	74.9	0.2		0.2	0.3	0.3		0.2	
[-120 ; -83]	11.6	68.1	0.2	19.8	0.1			0.1	0.1			
[-82 ; -53]	11.3	56.7	0.9	30.8	0.1			0.1	0.1			
[-52 ; -23]	11.0	45.8	1.5	41.1	0.1		0.1	0.2	0.2			
[-22 ; 7]	10.8	35.6	2.2	50.9			0.1	0.2	0.2			
[8 ; 18]	10.6	28.4	2.6	57.8			0.1	0.2	0.2		0.1	
[19 ; 79]	10.3	13.4	3.0	72.3	0.2		0.2	0.2	0.2		0.2	
[80 ; 119]	9.4	20.7	6.2	62.2	0.6			0.6	0.3			
[120 ; 199]	9.5	45.5	2.5	35.5	0.1		2.1	0.1	0.1		0.1	4.5
[200 ; 299]	8.9	42.3	2.7	36.3	0.1		3.0	0.1	0.1		0.1	6.4
[300 ; 399]	8.2	39.1	2.9	37.2	0.1		3.9	0.1	0.1		0.1	8.3
[400 ; 499]	7.6	36.1	3.0	38.0	0.1	0.1	4.7	0.2	0.1			0.1
[500 ; 599]	7.1	33.5	3.2	38.7	0.1	0.1	5.4	0.2				11.7
[600 ; 699]	6.6	31.0	3.3	39.4	0.1	0.1	6.1	0.2				13.2
[700 ; 799]	6.1	28.7	3.5	40.0	0.1	0.1	6.7	0.2				14.6
[800 ; 899]	5.6	26.5	3.6	40.5	0.1	0.2	7.3	0.3				15.9
[900 ; 999]	5.2	24.6	3.7	41.1	0.1	0.2	7.8	0.3				17.0
[1000 ; 1099]	4.9	22.7	3.8	41.6	0.1	0.2	8.3	0.3				18.1
[1100 ; 1199]	4.5	21.0	3.9	42.0	0.1	0.2	8.8	0.3				19.2
[1200 ; 1299]	4.2	19.4	4.0	42.5	0.1	0.2	9.2	0.3				20.1
[1300 ; 1399]	3.9	17.9	4.1	42.9	0.1	0.2	9.6	0.3				21.0
[1400 ; 1499]	3.6	16.5	4.2	43.2	0.1	0.2	10.0	0.3				21.9
[1500 ; 1599]	3.4	15.5	4.2	43.5	0.1	0.2	10.3	0.3				22.5
[1600 ; 1999]	3.4	15.5	4.2	43.5	0.1	0.2	10.3	0.3				22.5
[2000 ; 3060]	3.4	15.5	4.2	43.5	0.1	0.2	10.3	0.3				22.5
[3061 ;]												

B. Treatment head simulations

- Contribution of nuclear interactions in treatment head simulations (e.g. phase space calculations, fluence reduction, 'scattered' radiation); Review data on treatment head simulations and beam characterization from the open literature.

We have done simulations using a Geant4 implementation of the treatment head at MGH.

Secondary protons: For beam scanning, the contribution of secondary particles in the phase space can be entirely neglected. However, even for passive scattered proton beams, the contribution of secondary protons from the treatment head reaching the patient is pretty small. Secondary protons generated upstream of the final collimator are typically emitted at an angle preventing them to pass through the patient specific collimator. In addition, those generated within the collimator will most likely be stopped in it. For a very small aperture (diameter of the opening just 3 cm), the treatment head efficiency (protons exiting versus protons entering the treatment head) was simulated to be just 0.7%, while for a bigger aperture opening (15 cm diameter) it increased to 17.7% (2). The yield of secondary protons per primary proton in the phase space files was just 0.5% and 0.6%, respectively, i.e. pretty much independent of the field size [2]. Nuclear interactions do however play a role in the yield of the primaries as they cause loss of primary protons along the beam path through the treatment head.

Secondary neutrons: For patient dose calculations in treatment planning neutron doses are irrelevant. However, neutron doses are of concern regarding late effects of radiation therapy due to their elevated biological effectiveness at low doses. The amount of neutrons generated in a passive scattered treatment head is quite substantial. Again, for the two aperture scenarios given above, we determined that per proton in the phase space file, there are 4.3 and 0.2 neutrons, respectively, for these two examples. This number would certainly depend heavily on the used nuclear interaction cross sections. Most of the neutrons are of very low energy, i.e. can be expected to deposit very little dose in the patient. Specifically, roughly 1/3 is below 1 MeV and half are below 3 MeV.

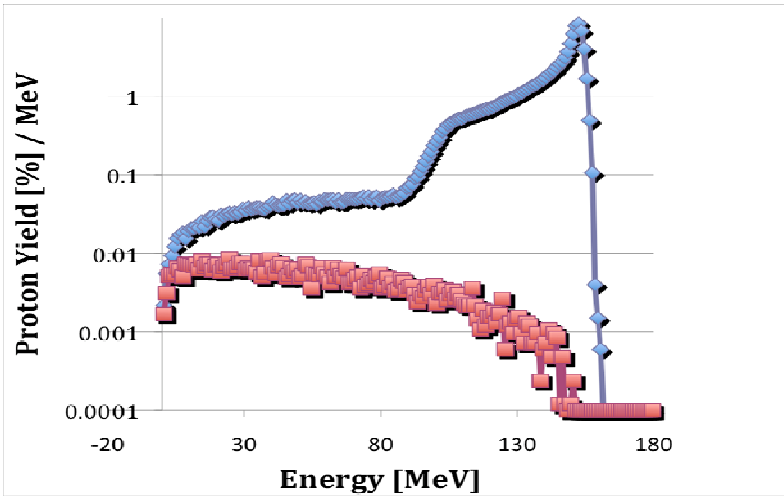

Fig. 1: Proton energy distribution at the exit of the treatment head for a field with a range of 16 cm in water and a modulation width of 10 cm at the Francis H Burr Proton Therapy Center at Massachusetts Genera Hospital (blue: primary protons; red: secondary protons from nuclear interactions) [2].

C. MLFC

- Comparison of different physics settings with experimental data from a Multi-Layer Faraday Cup (MLFC).

A multi-layer Faraday cup is an ideal tool to test for the total inelastic nuclear interaction cross section [3, 4]. We have tested various physics settings for proton beam therapy for target dose and secondary dose calculations using Geant4.8.1p01 [5]. We considered the simulation of electromagnetic and nuclear processes induced by proton beams with energies up to 250 MeV. Geant4 allows for the construction of a 'user physics list', i.e. a combination of 'processes' and 'models' that define the interaction probabilities and final state generation, respectively. Multiple Geant4 'processes' and 'models' can be assigned as alternatives to the same physical process in the user's application by means of a 'modular physics list', the actual physics setting being decided upon at run time.

A modular physics list was constructed to simulate the longitudinal charge development of a 160 MeV proton beam irradiating a stack of polyethylene absorbers and validate the simulation against measured distribution.

The models used in the 'reference physics list' were (see Fig. 2):

- standard electromagnetic model
- low-energy parameterized elastic model (G4LElastic) with the default elastic process (G4HadronElasticProcess)
- binary cascade model (G4BinaryCascade) for p,n inelastic scattering and a combination of binary cascade (G4BinaryLightIonReaction) and low-energy parameterized models (G4LEDeuteronInelastic, G4LETritonInelastic and G4LEAlphaInelastic) for the inelastic scattering of heavier hadrons

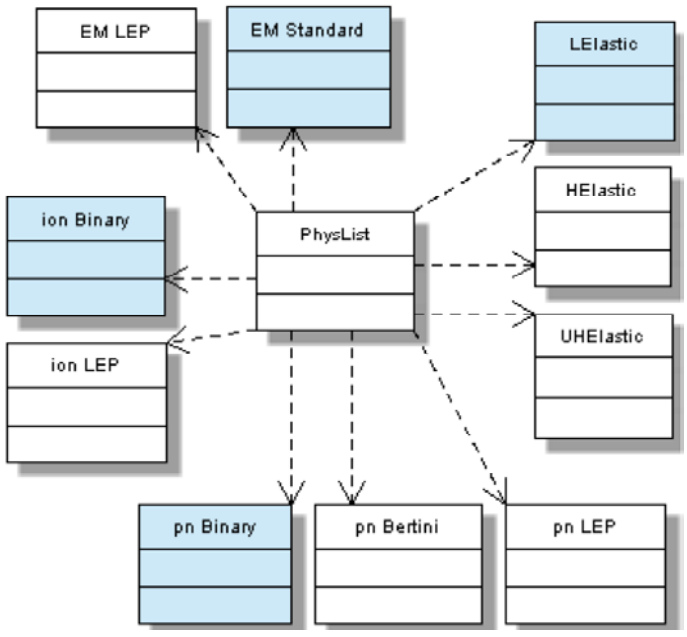

Fig. 2: Structure of the modular physics list used for the comparison of the Geant4 electromagnetic and nuclear interaction models. The modules of the reference physics list are highlighted.

The variants of the physics list were as to the following models/processes:

- low-energy parameterized electromagnetic model
- a variant LEP elastic model (G4HadronElastic) with the reference elastic process
- the reference elastic model with a variant elastic process (G4UHadronElasticProcess)
- Bertini cascade model for p,n inelastic scattering (G4CascadeInterface)
- low-energy parameterized models for p,n inelastic scattering (G4LEProtonInelastic, G4LENeutronInelastic)
- low-energy parameterized models (exclusively) for ion inelastic scattering

The standard electromagnetic model was found to be more suitable than the low-energy parameterized. The nuclear p,n inelastic low-energy parameterized model was rejected in the validation process, leaving the binary and Bertini cascades as two candidates, the former giving more accurate results. The nuclear de-excitation model parameters were found to have no significant effect on the simulation; the default model settings were hence used. Due to improved cross-section for the elastic scattering of protons and neutron on hydrogen, the new elastic scattering process of Geant4 was opted for.

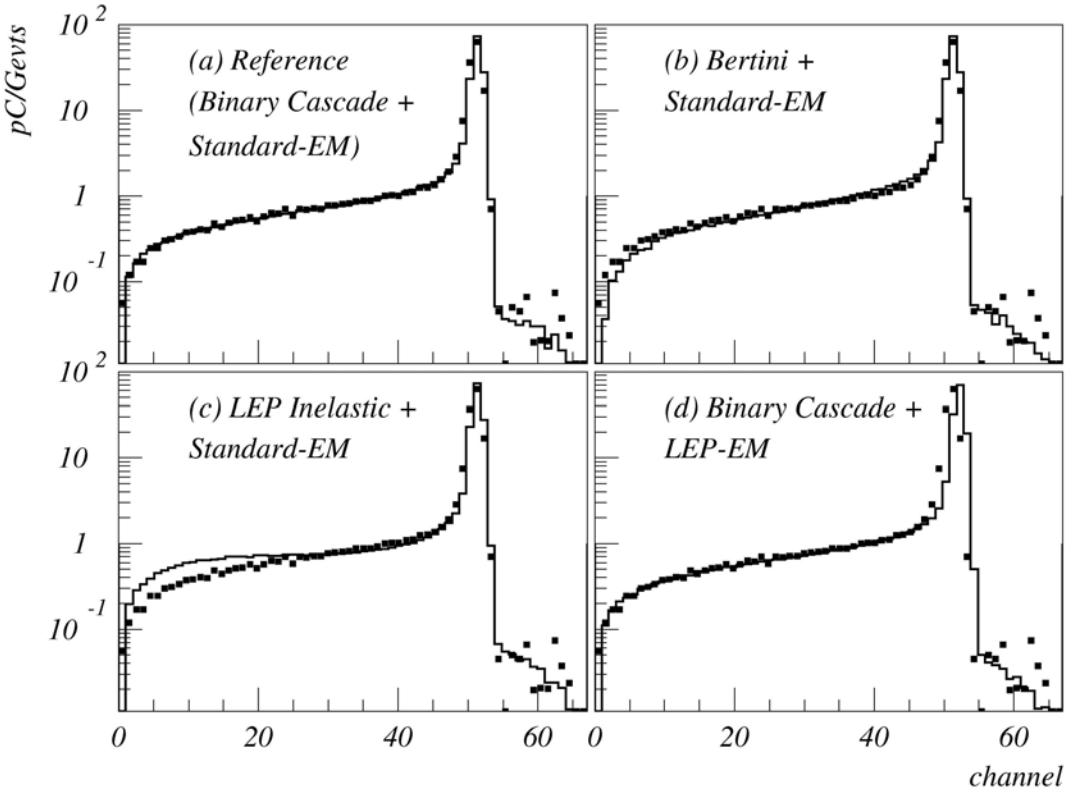

Fig. 3: Comparison of measured and simulated longitudinal charge distributions in the Faraday cup for (a) the reference physics list and three variations evaluating (b) the Bertini model for p,n inelastic scattering, (c) the low-energy parameterized model for p,n inelastic scattering and (d) the low-energy parameterized model of electromagnetic interactions. The simulated (measured) distributions are shown by the histograms (squares), respectively. The horizontal axes show the charge collector ('channel') number (with increasing depth) in the Faraday cup. The vertical axes show the collected charge normalized to the number of protons in the beam [5].

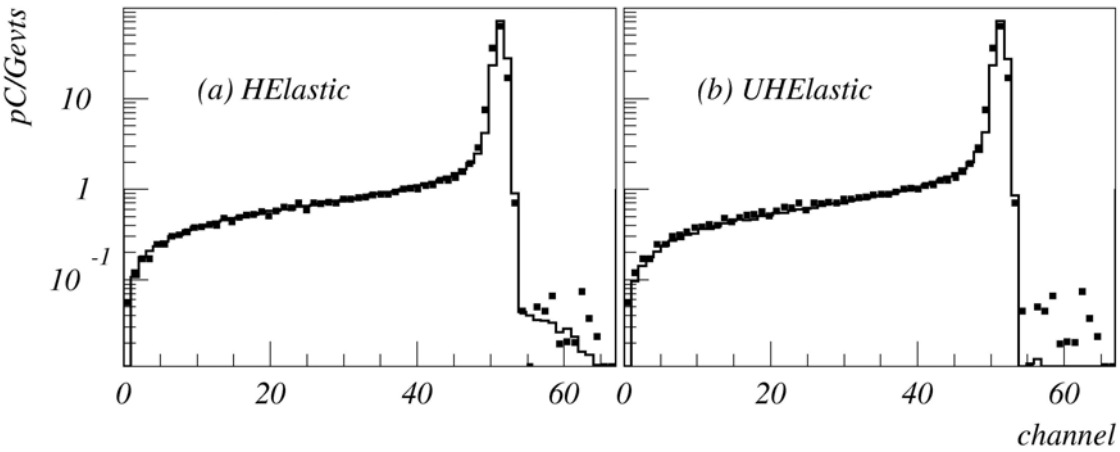

Fig. 4: Comparison of measured and simulated longitudinal charge distributions in the Faraday cup for two variants of the reference elastic model: (a) G4HadronElastic model with default hadron elastic process (b) G4HadronElastic model with the unified hadron elastic process. The simulated (measured) distributions are shown by the histograms (squares), respectively. The horizontal axes show the charge collector ('channel') number (with increasing depth) in the Faraday cup. The vertical axes show the collected charge normalized to the number of protons in the beam [5].

- MLFC data will be provided for users of other codes (MCNPX, SHIELD-HIT, FLUKA) for running similar comparisons. SHIELD-HIT has been benchmarked against the MLFC data as well [6].

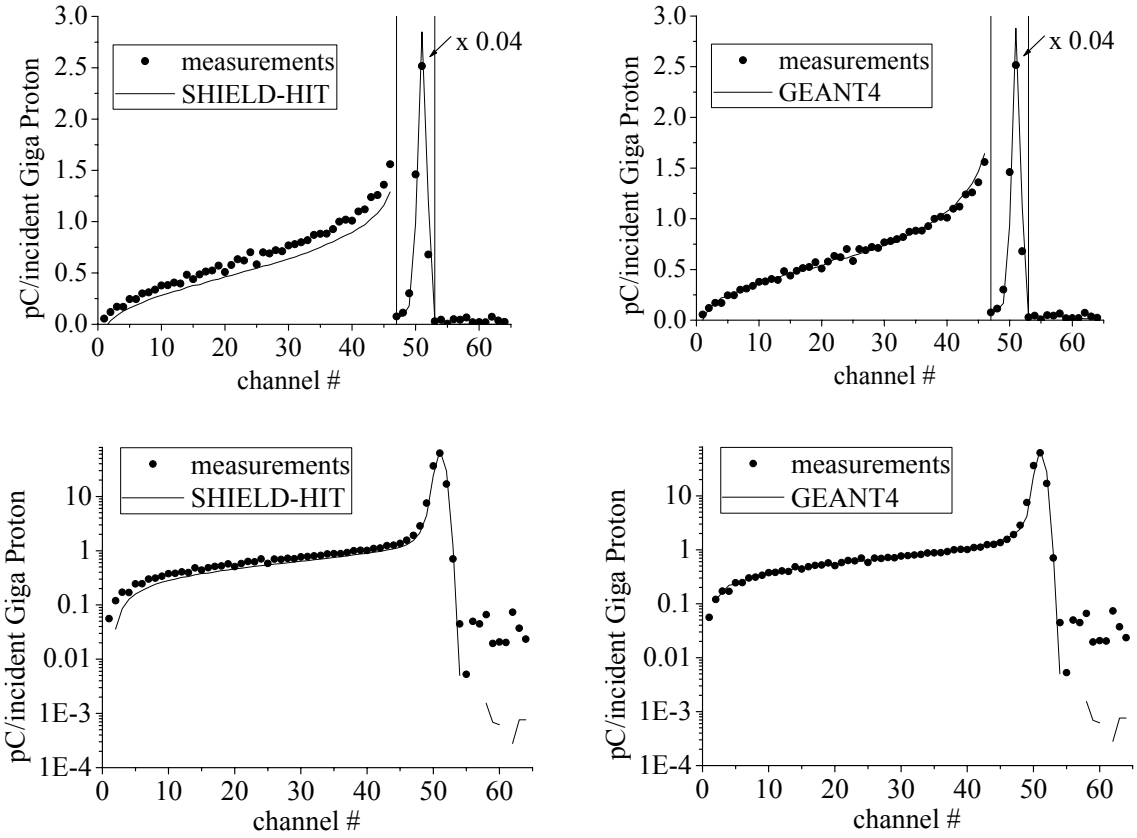

Fig. 5: SHIELD-HIT (left) and GEANT4 (right) calculations (line) and experiment (circles). The ordinate shows absolute values and the abscissa is the channel number [6] .

D. Neutrons

- Sensitivity of different neutron data (or model settings) on dose, neutron energy distributions, and equivalent dose

  Neutron energy distributions not only determined the dose deposited indirectly by neutrons, but also the associated radiation quality factor to assess the side effects of neutron exposure in radiation therapy

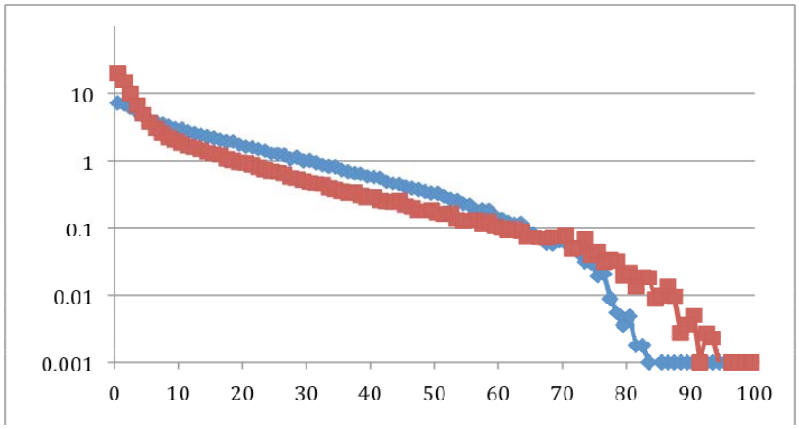

Fig. 6: Neutron emission energy distributions for water (red) and brass (blue). Water may represent tissue whereas brass may represent the treatment head contributions.

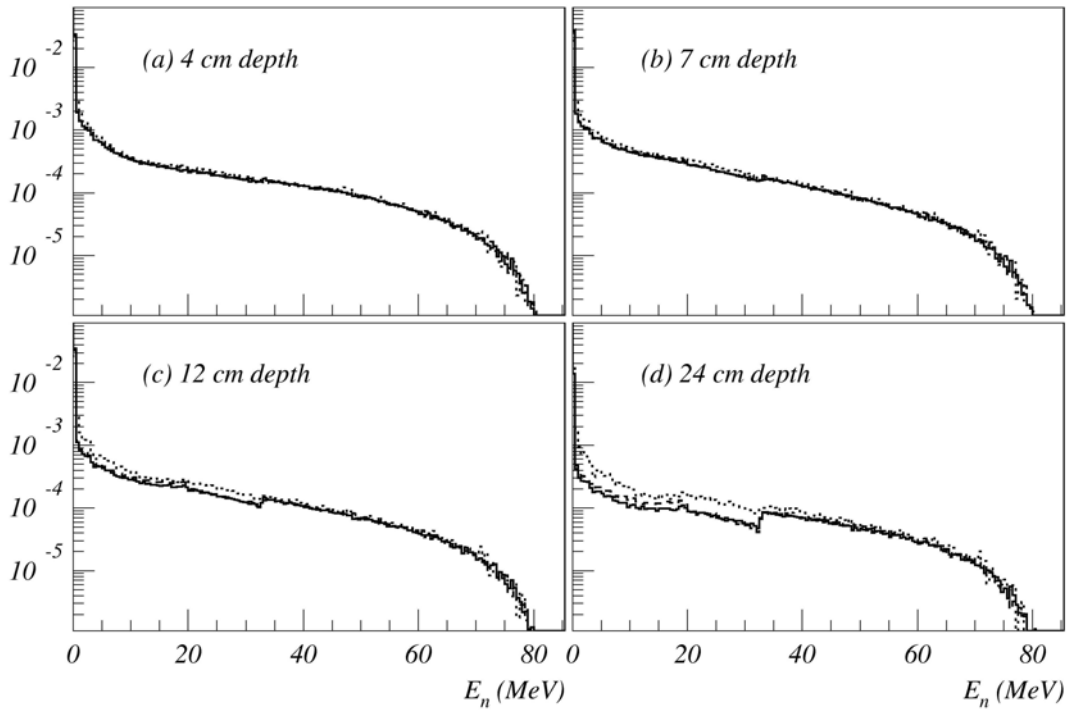

Fig. 7: Comparison of neutron energy distributions between the reference physics list (solid histograms) and two alternative elastic nuclear scattering models: G4HadronElastic model with default hadron elastic process (dashed histograms) and G4HadronElastic model with the unified hadron elastic process (dotted histograms). The plots show energy distributions at (a) 4 cm, (b) 7 cm, (c) 12 cm and (d) 24 cm depth in a water phantom irradiated by a 10 x 10 cm 100 MeV proton field [5].

- Comparison of MGH data on Bonner sphere measurements and microdosimetric measurements with Geant4 Monte Carlo simulations based on reference physics list.

The neutron detectors used were 10” equivalent Bonner spheres, which were set to record total counts due to neutrons. These Bonner spheres consist of a proportional chamber filled with BF3 gas at the center of polyethylene sphere 9” in diameter plus some Cd to act like a 10” Bonner sphere. The polyethylene moderates the neutrons to thermal energies, which are detected by the proportional chamber via the reaction $^{10}B(n,\alpha)^{7}Li$. The Bonner spheres were calibrated by measuring the response when the detector was placed 1 meter from an Am/Be source of known activity. The quality factor of the neutrons from the Am/Be source was assumed to be eight. The number of counts collected by each Bonner sphere was automatically dumped every two seconds to a small laptop computer located remotely outside the treatment rooms.

A water tank (30x30 cm) positioned such that the center of the spread out Bragg peak (SOBP) was at isocenter simulated the patient. The beam was stopped either in a brass block at the patient aperture position before the water tank or in the water tank when an open field was used. Measurements at 3 different distances to isocenter 40, 80 and 120 cm were made at 4 angles to the treatment beam, 0^{o}; 90^{o}; 45^{o}; and 45^{o} in the backward direction. Three Bonner spheres were used at each angle. Later measurements were required to determine the correction factors for those Bonner spheres operating in the shadow of upstream Bonner Sphere(s).

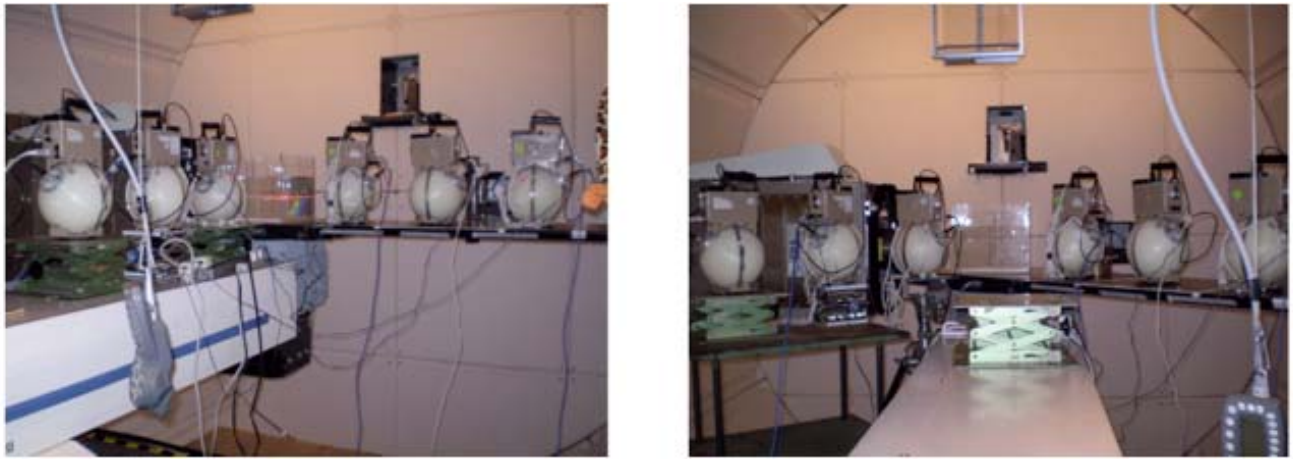

Fig. 8: Arrangement of the Bonner sphere detectors in the treatment rom. The beam nozzle is seen on the right side in the pictures.

Results are shown in Fig. 9 [2].

Further, measurements were done with a thimble ionization chamber and the Wellhofer MatriXX detector inside a Lucite phantom with field configurations based on the treatment of prostate cancer and medulloblastoma as shown in Fig. 10. We used GEANT4 to simulate fields delivered in the measurements. The partial contributions to the dose are separated in the simulation by particle type and origin [7].

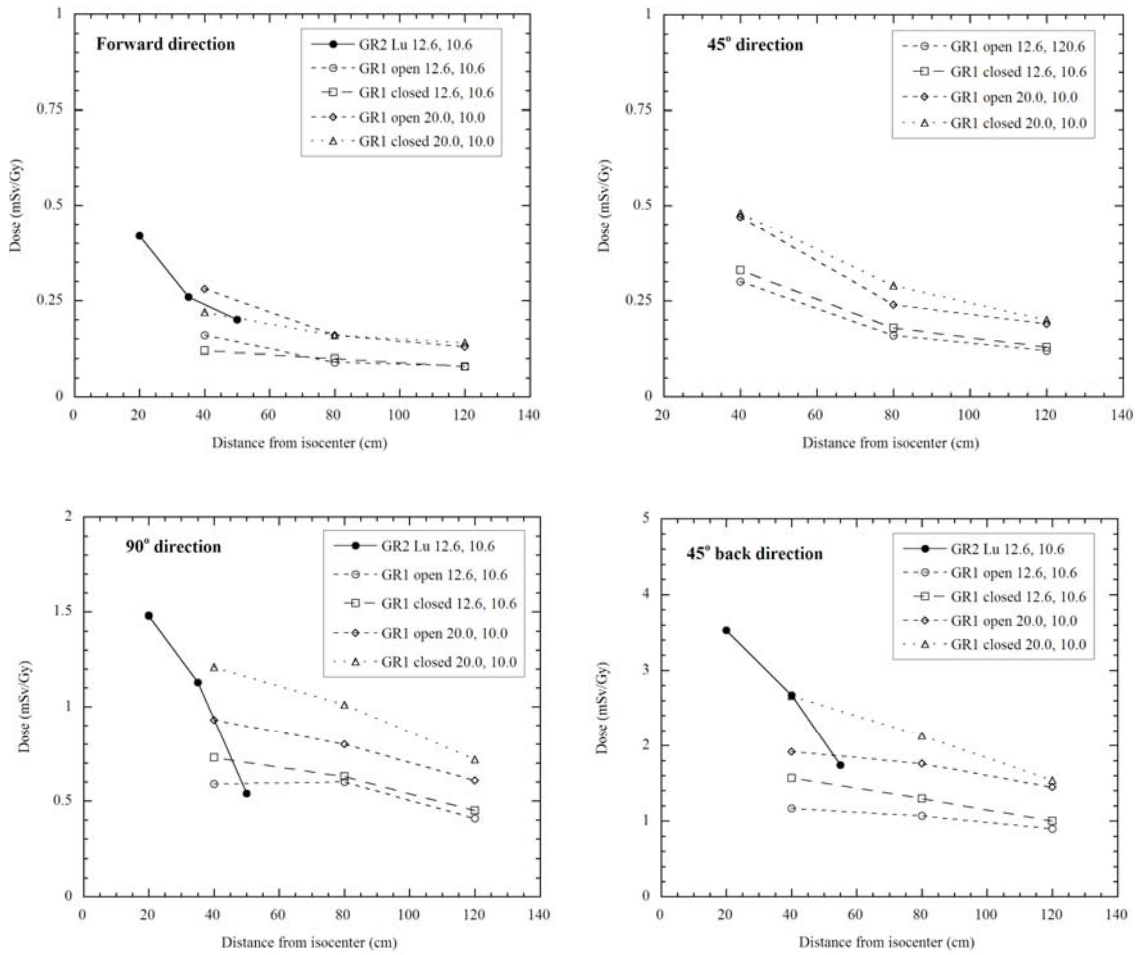

Fig. 9: Neutron doses in mSv/Gy for different angles relative to the beam direction as measured using the Bonner sphere detectors in the treatment room.

The agreement between the experiment and simulation in the out-of-field absorbed dose is within 30% at 10 to 20 cm from the field edge and 90% of the data agrees within 2 standard deviations as can be seen in Fig. 11. In passive scattering, the neutron contribution to the total dose dominates in the region downstream of the Bragg peak (65 to 80% due to internally produced neutrons) and inside the phantom at distances more than 10-15 cm from the field edge. The equivalent dose at 15-20 cm from the field edge decreases with depth in passive scattering and increases with depth in active scanning. We confirm that there is a reduction in the out-of-field dose in active scanning but the effect decreases with depth. Depending on the position, the absorbed dose outside the primary field is dominated by contributions from primary protons that may or may not have scattered in the brass collimating devices and their associated delta electrons, photons and fragments from nuclear reactions that do not generate neutrons. GEANT4 is suitable for simulating the dose deposited outside of the primary field.

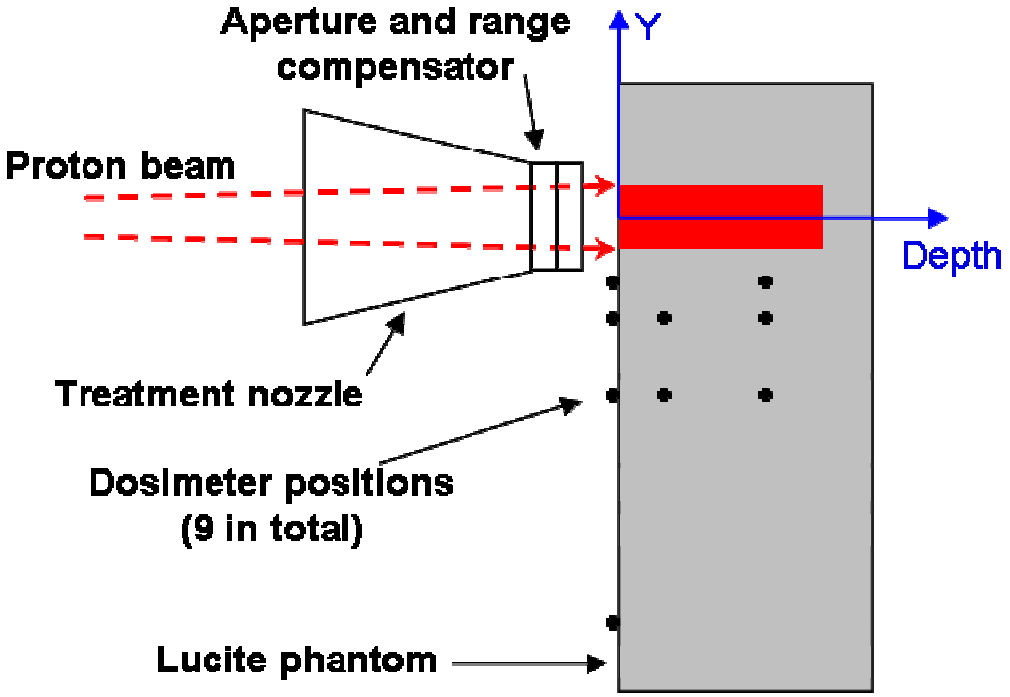

Fig. 10: Configuration of the nozzle and phantom and positions of the dosimeter in the horizontal plane. The dark gray region (red in color) shows the primary field in the phantom. The dosimeter was positioned at 5, 10, 20 and up to 60 cm lateral to the field edge (black, solid circles).

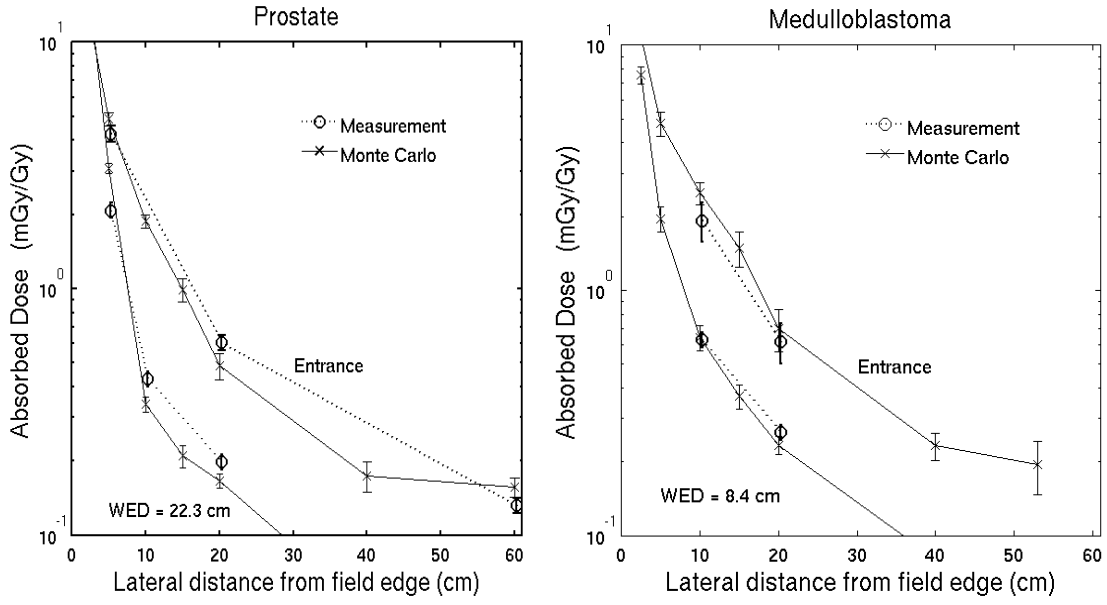

Fig. 11: Simulated and experimental dose for (a) the passively scattered prostate cancer field and (b) the cranial medulloblastoma field. Data points are offset slightly for clarity. The data verify the suitability of the Monte Carlo model.

E. Patient Dose

- Simulations for different field parameters and different geometries (head and neck with bony structures versus soft tissue cases) to study the contribution of nuclear interaction products to the dose distribution.

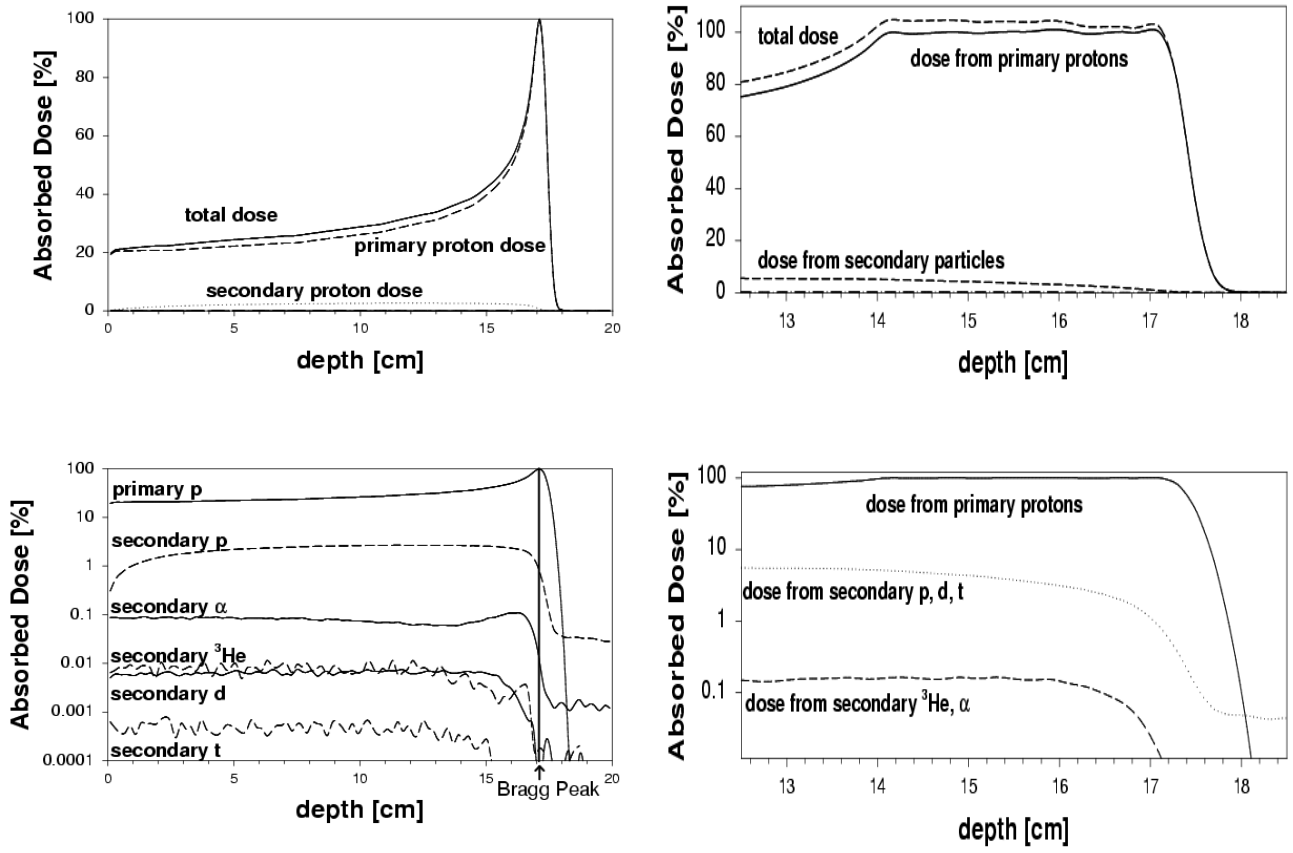

Fig. 12: Depth dose distributions (Bragg peak normalized to 100%) for a proton beam incident on a water phantom. The upper figure shows the total dose and the dose due to primary and secondary protons. The lower figure compares, on a logarithmic scale, the doses due to different types of particles (solid lines: primary p, secondary α and d; dashed lines: secondary p, ^{3}He, t). A vertical line indicates the position of the maximum of the Bragg peak. Left side: 160-MeV proton beam; right side: modulated 160-MeV proton beam. The dose is laterally summed to the limits of the dose plateau (± 3cm) [8] .

The impact of secondary particles on depth dose curves is well known and several investigators have published on this effect. We did look at the influence of model variations with respect to depth-dose curves in water comparing with measured data as shown in Fig. 13. The influence of nuclear interactions may be smaller in the patient because of the geometrical inhomogeneity washing out effects.

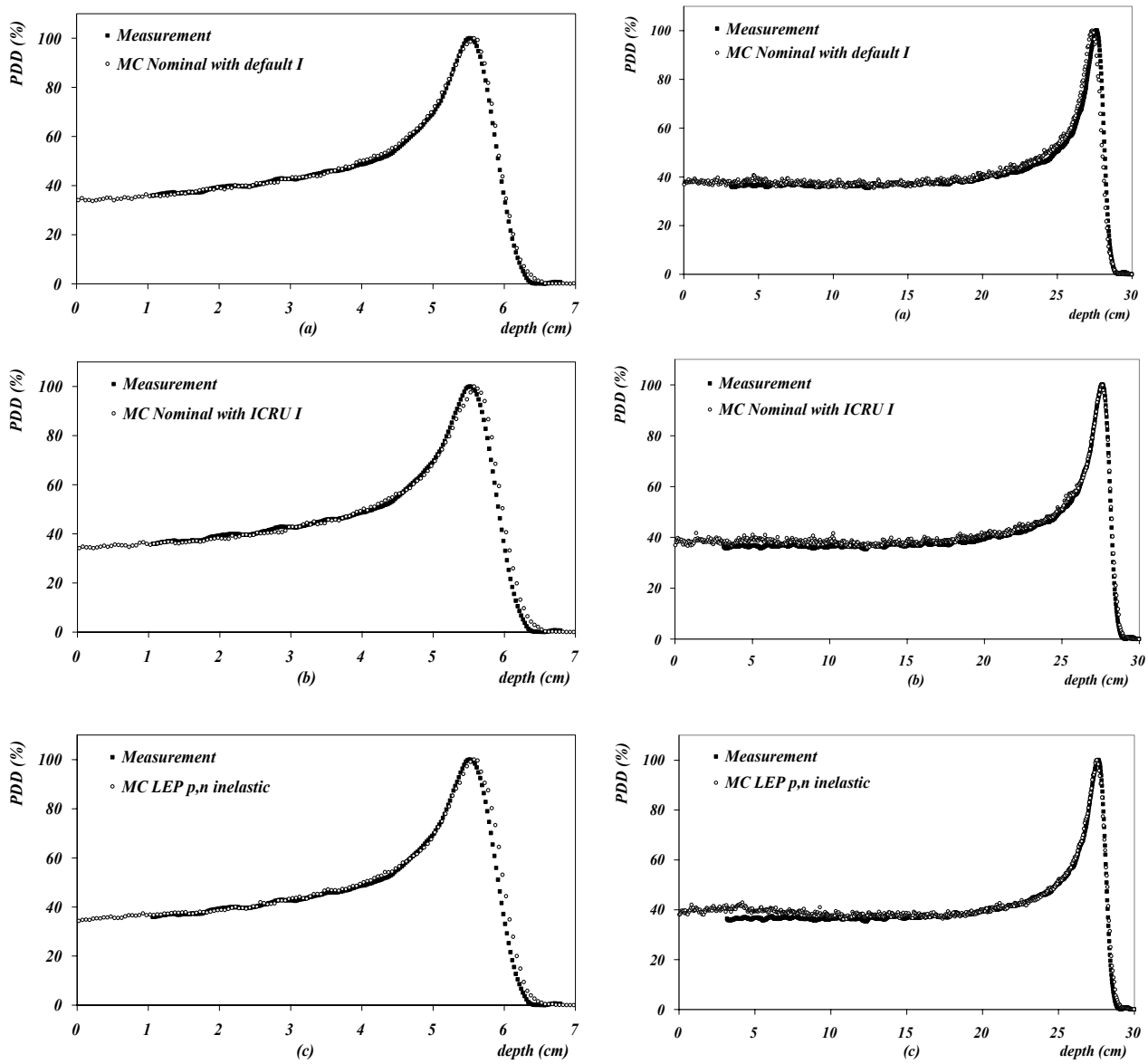

Fig. 13: Measured (squares) and simulated (circles) percent depth-dose distributions in water for a low energy proton beam and (a) the nominal physics list with the default ionization potential, (b) the nominal physics list with the ICRU ionization potential and (c) a variant of the nominal physics list using the low-energy parameterized model for p,n inelastic scattering. Left: low-energy proton beam; right: high-energy proton beam [5].

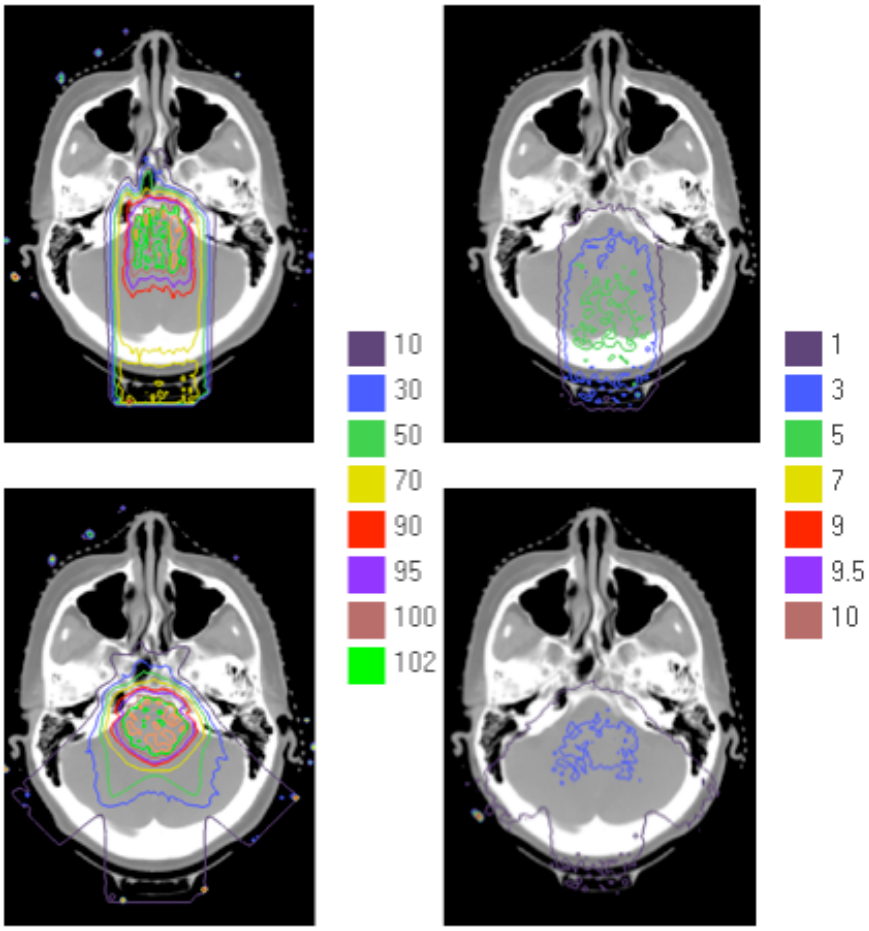

Fig. 14: Results of a Monte Carlo dose calculation for a patient with a spinal cord astrocytoma. Left side: total absorbed dose, right side: absorbed dose due to secondary protons only. Upper row: one field, lower row: all 3 treatment fields [2] .

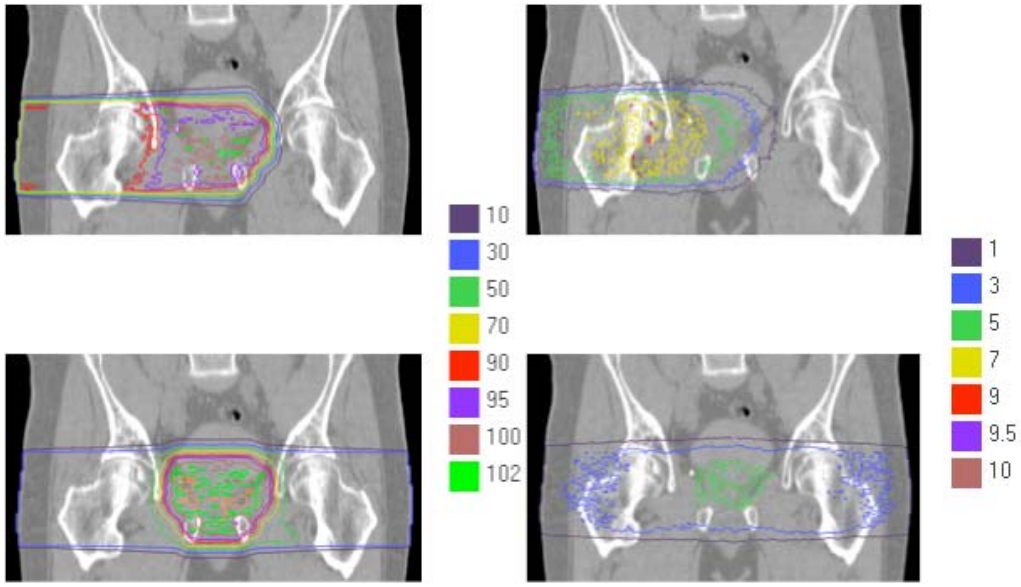

Fig. 15: Results of a Monte Carlo dose calculation for a patient with prostate cancer. Left side: total absorbed dose, right side: absorbed dose due to secondary protons only. Upper row: one field, lower row: all 2 treatment fields [2] .

- Nuclear interaction when converting doses

Dose in radiation therapy is traditionally reported as water-equivalent dose, or dose to water. Monte Carlo dose calculations report dose to medium and thus a methodology is needed to convert dose to medium into dose to water (or vice versa) for comparison of Monte Carlo results with results from planning systems.

We developed a formalism to convert dose to medium into dose to water for proton beam dose calculations. Three different methods were introduced, an approximate method based on energy independent relative stopping powers which allows retro-active conversion, a method considering energy dependent relative stopping powers, and a method incorporating nuclear interaction events. Luckily, we found that the difference between the three methods was within 1% in most cases when analyzing doses to contoured structures. Nevertheless, we present the correct method here.

To consider energy deposition in nuclear interactions to convert dose to tissue D_m (from Monte Carlo) into dose to water D_w, an additional term has to be introduced as was shown by Palmans and Verhaegen [9]:

$$D_m = D_w^{Coulomb} \times s_{m,w}(E) + D_w^{Nuclear} \times \left(E_{trans} \sigma_{react}(E) \Big/ A \right)_{m,w} \quad (1)$$

The additional term deals with energy deposited in nuclear interactions. The secondary particles, if loosing energy electromagnetically, would be included in the first term. The additional term depends on the energy of the primary particle E, the cross sections for nuclear interactions, σ_{react}, and the atomic number A of the different media. The energy transferred to the recoil (assuming that all other secondaries are being tracked), E_{trans}, takes into account that not only the cross section but also the energy transferred is material dependent. Eq. (1) holds not only if the dose from nuclear interactions is deposited locally [9], but also if secondary particles are tracked under the condition of charged particle equilibrium. Thus, independent of whether secondary particles are tracked or not, a conversion from D_m to D_w in proton radiation dosimetry (e.g. with ionization chambers) can be done accurately applying Eq. (1).

For converting D_m to D_w for Monte Carlo dose calculation, the above equation is strictly only an approximation [10]:

$$D_w^{Nuclear} = D_m^{Nuclear} \times \left(E_{trans} \sigma_{react} (E) \Big/ A \right)_{w,m} \times (1 - \Phi_{w,m}) \ldots\ldots (2)$$

Note that this equation corrects for the difference in energy deposited locally without taking into account the difference in energy given to secondary particles ($\Phi_{w,m}$).

In our case, all nuclear interaction products were considered, with the exception of gammas, electrons, neutrons and protons because they are explicitly tracked. This implies that the application of the nuclear interaction correction term in the equation depends on the Monte Carlo algorithm, i.e. which secondary particles are being tracked (the definition of D_w might even depend on the algorithm implemented in the planning system to which the Monte Carlo dose is compared. It depends, for example, on the implementation of the $\Phi_{w,m}$ fluence reduction due to nuclear interactions).

In principle, secondary particles in a Monte Carlo simulation can easily be identified by setting a boolean flag. This preserves the information of a parent-daughter relationship for each particle. The cross section as well as the energy transferred to tissue is known within the Monte Carlo at each interaction point. The problem with $\Phi_{w,m}$ is that it would require keeping track of all nuclear interactions along the path of each particle, i.e. the integral over the particle production cross sections along the particle path over all media. The amount of book-keeping would be significant in terms of memory consumption and computational efficiency. Alternatively one could define an "effective" stopping power for the entire proton spectrum, including primary and secondary protons [11].

As first order approximation, we neglect the fluence correction, which leads to the conversion scheme considering energy dependent relative stopping power and nuclear interactions, D_w^C:

$$D_w^c = [D_m \times s_{w,m}(E)]_{proton} + [D_m \times s_{w,m}(E)]_{electron} + D_m^{Nuclear} \times \left(E_{trans}\sigma_{react}(E) \Big/ A \right)_{w,m} \quad \ldots\ldots(3)$$

For the nuclear interaction term the average energy transfer (averaged over all nuclear interaction processes) was simulated and fitted the data with two 3rd order polynomials. Fig. 16 shows the results for tissues 4, 8, 12, 16, 20, and 24. There is some fine structure in the transferred energy versus the incident proton energy. This is most pronounced in the low energy region (< 20 MeV). There is also a small 'hump' near ~35 MeV (not detectable in the figure). These effects are due to nucleon-nucleon collisions following proton induced inelastic interactions [12]. Note that the correction factor for tissue 8 does no longer fall for all energies between the curves for tissues 16 and 20. This is because the energy transferred depends mainly on the mass of the target nuclei.

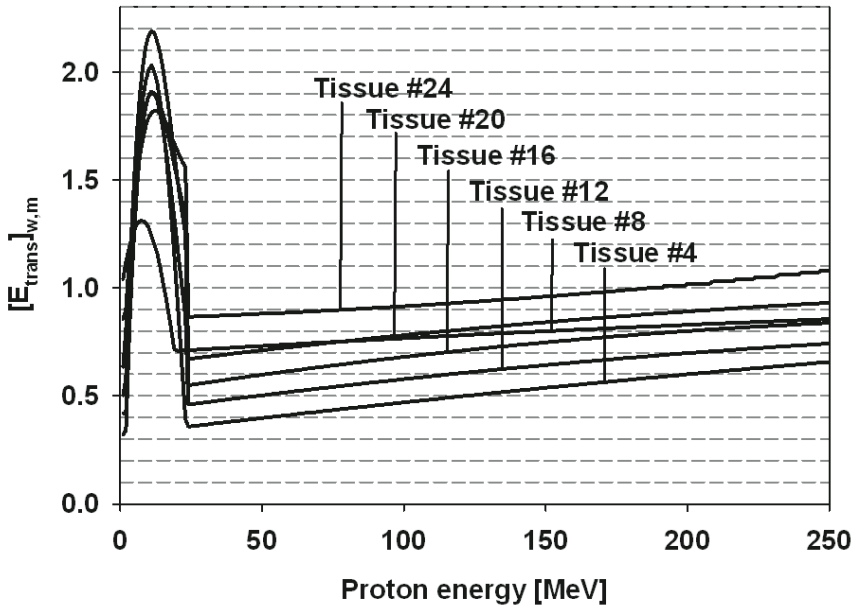

Fig. 16: Ratio of energy transferred into kinetic energy of particles other than gammas, electrons, neutrons and protons in water versus tissue.

To determine the reaction cross sections as a function of elemental composition and atomic mass we used the parameterization by Tripathi *et al* [13, 14].

$$\sigma_{react} = \pi r_0^2 \times \left(A_{proton}^{1/3} + A^{1/3} + \delta_E \right)^2 \times \left(1 - B/E_{cm} \right) \tag{4}$$

Here, r_0^2 equals 1.1 fm, r_{rms} is the equivalent square radius (equals $r_0 \times A^{1/3}$), δ_E and B are constants, and E_{cm} is the center of mass kinetic energy of the colliding system (i.e. E_{cm} equals $m_{target}/(m_{proton}+m_{target}) \times E$). The term on the right side corrects for Coulomb interactions, which become significant at lower energies.

$$B = 1.44 \times Z \times \left[1.29 \left(r_{rms}^{proton} + r_{rms}^{target} \right) + \frac{1.2 \left(A_{proton}^{1/3} + A^{1/3} \right)}{E_{cm}^{1/3}} \right]^{-1} \tag{5}$$

$$\delta_E = 1.85 \frac{A_{proton}^{1/3} \cdot A^{1/3}}{A_{proton}^{1/3} + A^{1/3}} + \left(\frac{0.16 \frac{A_{proton}^{1/3} \cdot A^{1/3}}{A_{proton}^{1/3} + A^{1/3}}}{E_{cm}^{1/3}} \right) - C_E + \left[0.91 \frac{(A - 2Z)}{A_{proton} \cdot A} \right] \tag{6}$$

$$C_E = 2.05 \times \left[1 - \exp\left(-E/40 \right) \right] - 0.292 \exp\left(-E/792 \right) \times \cos\left(0.229 E^{0.453} \right) \tag{7}$$

For compounds consisting of i elements with fractions by weight w_i we can calculate:

$$\left(\sigma_{react}(E)/A \right)_{compound} = \sum w_i \times \left(\sigma_{react}(E)/A \right)_i \tag{8}$$

This leads to Fig. 17.

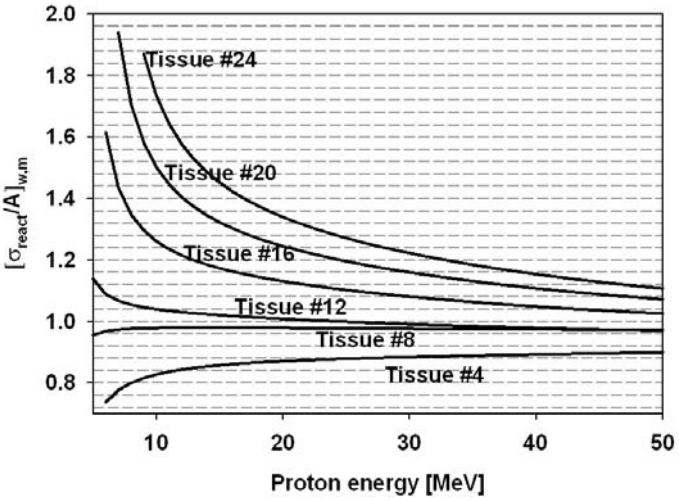

Fig. 17: Ratio of the reaction cross section, $[\sigma_{react}/A]_{w,m}$, for tissues 4, 8, 12, 16, 20, and 24 from table 1.

References

[1] Paganetti H., Jiang H., Parodi K.*, et al.,* Clinical implementation of full Monte Carlo dose calculation in proton beam therapy. *Phys Med Biol* 2008;53:4825-4853.

[2] Paganetti H., unpublished data. 2009.

[3] Gottschalk B., Platais R., Paganetti H., Nuclear interactions of 160 MeV protons stopping in copper: a test of Monte Carlo nuclear models. *Medical Physics* 1999; 26:2597-2601.

[4] Paganetti H., Gottschalk B., Test of Geant3 and Geant4 nuclear models for 160 MeV protons stopping in CH_2. *Medical Physics* 2003; 30:1926-1931.

[5] Zacharatou Jarlskog C., Paganetti H., Physics settings for using the Geant4 toolkit in proton therapy. *IEEE Transactions in Nuclear Science* 2008; 55:1018-1025.

[6] Henkner K., Sobolevsky N., Paganetti H., Test of the nuclear interaction model in SHIELD-HIT and a dose comparison with GEANT4. *Medical Physics* 2009; conditionally accepted for publication.

[7] Clasie B., Wroe A., Kooy H.*, et al.,* Experimental and theoretical assessment of out-of-field absorbed dose in proton fields. *Medical Physics* 2009; submitted for publication.

[8] Paganetti H., Nuclear Interactions in Proton Therapy: Dose and Relative Biological Effect Distributions Originating From Primary and Secondary Particles. *Physics in Medicine and Biology* 2002; 47:747-764.

[9] Palmans H., Verhaegen F., Assigning nonelastic nuclear interaction cross sections to Hounsfield units for Monte Carlo treatment planning of proton beams. *Physics in Medicine and Biology* 2005; 50:991-1000.

[10] Paganetti H., Dose to water versus dose to medium in proton beam therapy. *Physics in Medicine and Biology* 2009; in press.

[11] Laitano R.F., Rosetti M., Frisoni M., Effects of nuclear interactions on energy and stopping power in proton beam dosimetry. *Nuclear Instruments and Methods A* 1996; 376:466-476.

[12] Tripathi R.K., Cucinotta F.A., Wilson J.W., A simple method for nucleon-nucleon cross sections in a nucleus. *NASA Technical Paper* 1999;TP-1999-209125.

[13] Tripathi R.K., Cucinotta F.A., Wilson J.W., Accurate universal parameterization of absorption cross sections. *Nuclear Instruments and Methods in Physics Research B* 1996; 117:347-349.

[14] Tripathi R.K., Cucinotta F.A., Wilson J.W., Universal parameterization of absorption cross sections. *NASA Technical Paper* 1997;3621.

2.2. H. Palmans (NPL)

The application topics of the activities by NPL are graphite calorimetry (graphite to water dose conversion, perturbation factors), total absorption calorimetry and ionisation chamber dosimetry (perturbation correction factors). Experimental work has mainly concentrated on the graphite to water dose conversion.

People involved in this work are:

- Leena Al-Sulaiti / PhD student Univ. Surrey: Analytical modelling, MCNPX simulations and experiments on water equivalence graphite, aluminium, PMMA, A150, copper
- Russell Thomas / NPL: Experiments water equivalence and ion chamber response
- David Shipley / NPL: Geant4 simulations water equivalence, calorimeter perturbations, Faraday cup

- Mark Bailey and Florian Gabler / NPL: Calorimeter construction and measurements
- Franscesca Fiorini / PhD student Univ Birmingham: FLUKA simulations calorimeter perturbations (she is also performing FLUKA simulations of activation)

1. Calorimeter construction

New portable primary standard level graphite calorimeter construction has been delayed by approximately one year but is now well underway to completion. Once the calorimeter is operational it will be commissioned and compared to existing photon calorimeter in NPL, followed by a test run at CCO comparing with previous data from prototype calorimeter:

Portable design:

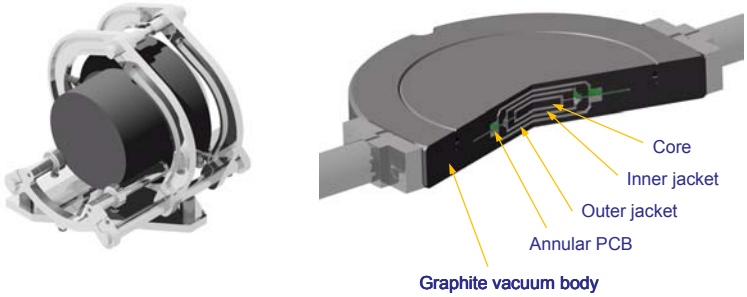

2. Measurements on graphite to water dose conversion in 60 MeV CCO beam

2.1. Broad beam comparison graphite and water

Tissue Phantom Ratio (TPR) measurements in graphite have been compared with TPR measurements derived from Percentage Depth Dose (PDD) in water.

Schematic set-up:

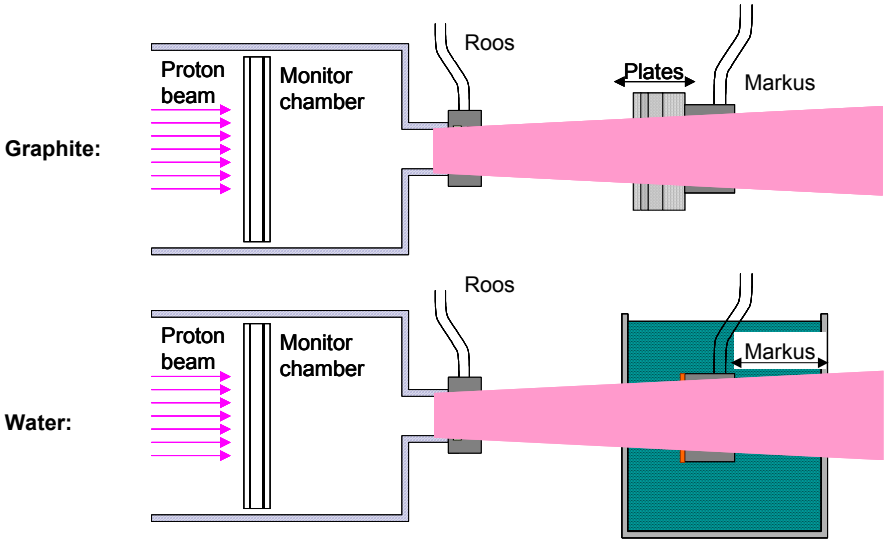

Roos chamber serves as monitor. In graphite Markus ion chamber was kept at constant SDD at isocentre, in water PDD were measured with surface at isocentre. Water phantom entrance window = mica. The water protecting PMMA cap of the Markus chamber has been accounted for. PDD in water was converted to TPR using inverse square law using SDD of 1800 mm. The water equivalent thickness of the Roos chamber was found to be 2.9 mm. For the in-water measurements a point at the surface could not be measured but it could be extrapolated from the measurements without the Roos chamber present. This means that the point at zero depth has a different meaning for graphite and water.

TPR results in water and graphite for pristine (left) and full-modulated (right) beams:

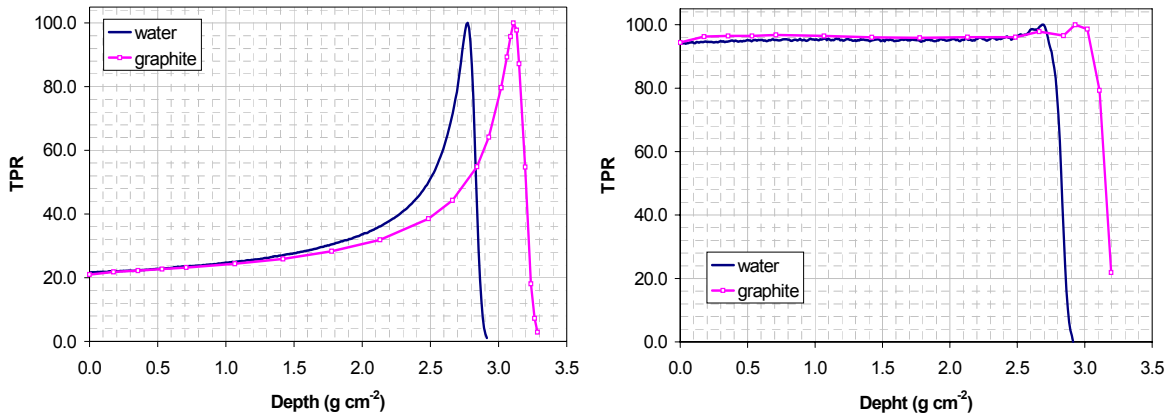

Range scaling is performed at 50% or 80 % of D_{max} at distal edge or by using ICRU Report 49 data.

Resulting fluence correction for pristine (left) and full-modulated (right) beams:

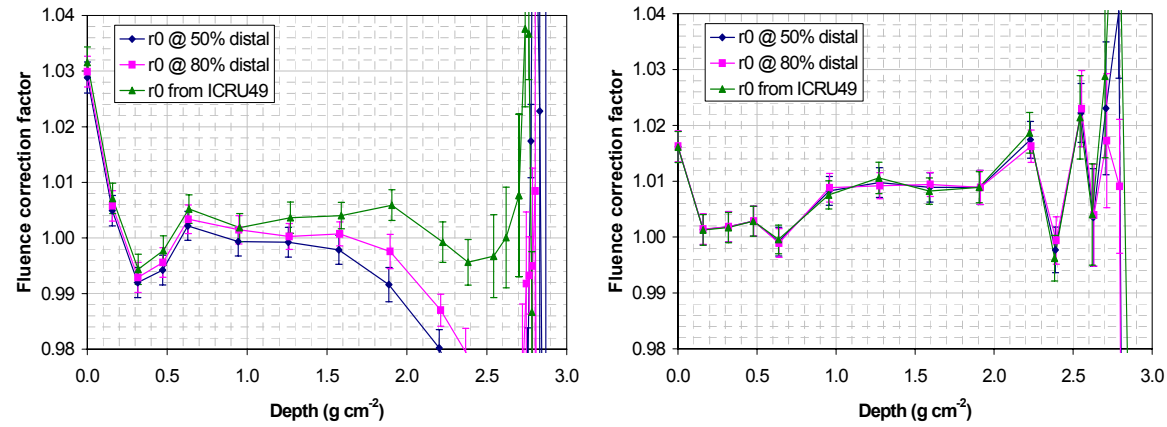

The uncertainty bars include type A + type B uncertainties for propagation of the uncertainty on the mass thickness of the graphite plates through the depth conversion. Due to the latter contribution the uncertainty becomes larger in the Bragg peak region, where the fluence gradient is larger.

2.2. Narrow beam comparison graphite and water

Schematic set-up:

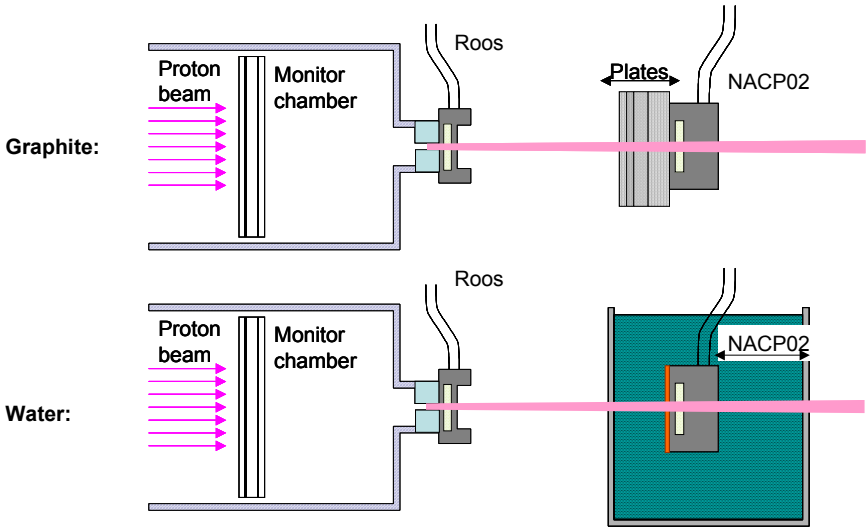

The beam diameter was 4 mm. The NACP02 chamber was chosen since it will cover the entire beam laterally. There should be no r^{-2} correction and TPR can be directly compared with PDD. For the rest similar as for broad beam experiment.

Resulting fluence correction without any correction for pristine (left) and full-modulated (right) beams:

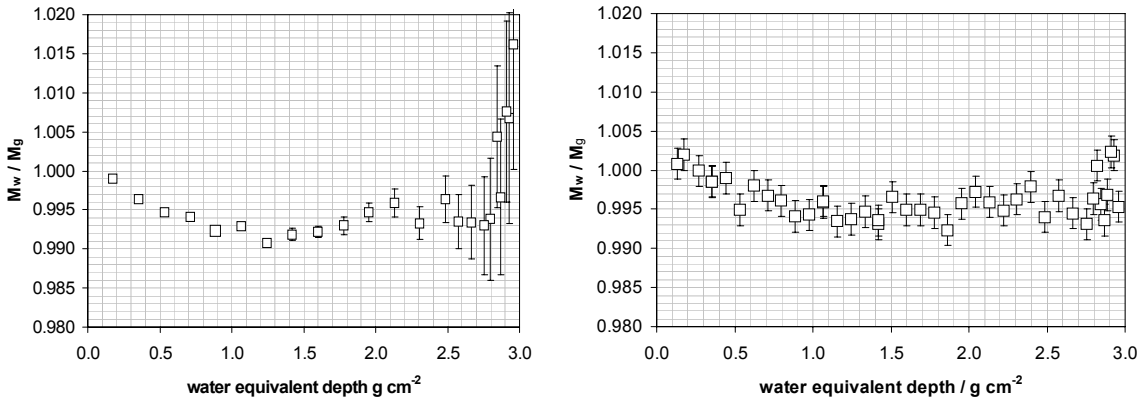

But, absence of distance correction for the water measurements was tested at a few distances for pristine (left) and full-modulated (right) beams:

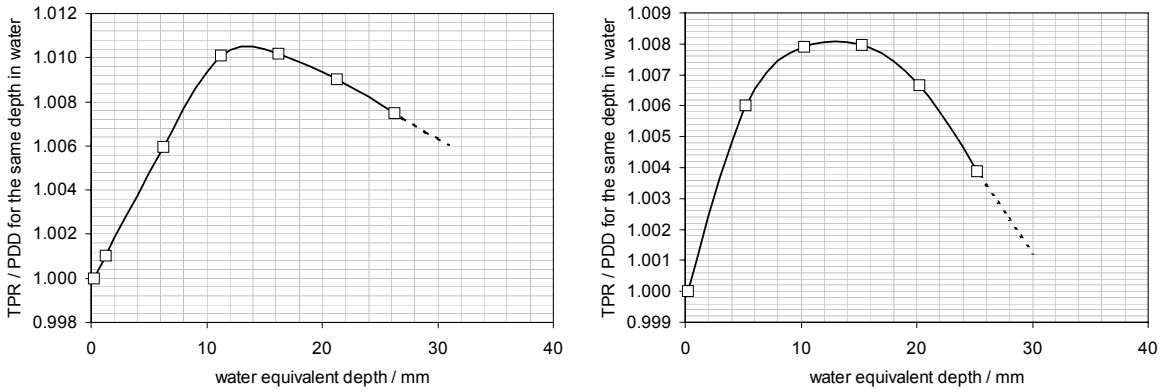

Resulting fluence correction after correction for pristine (left) and full-modulated (right) beams:

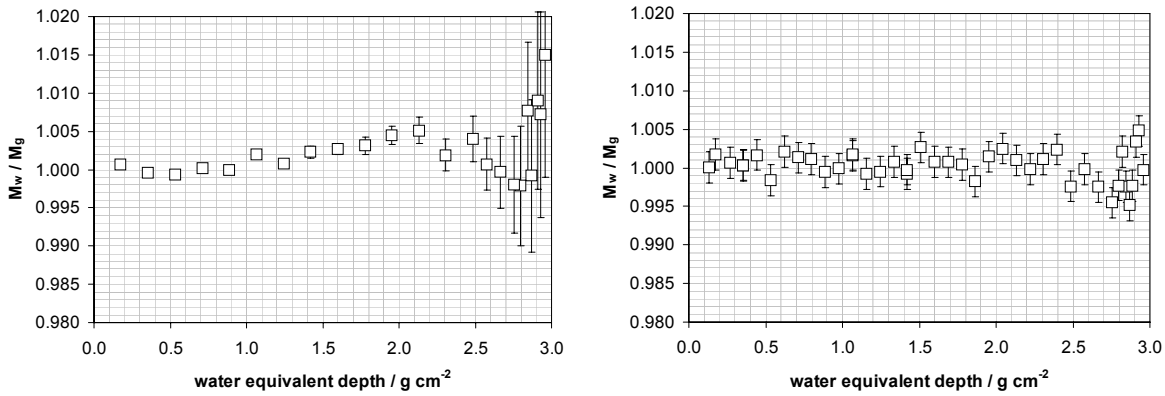

2.3. Narrow beam comparison between other materials and water

Resulting fluence correction for A150 after correction for pristine (left) and full-modulated (right) beams:

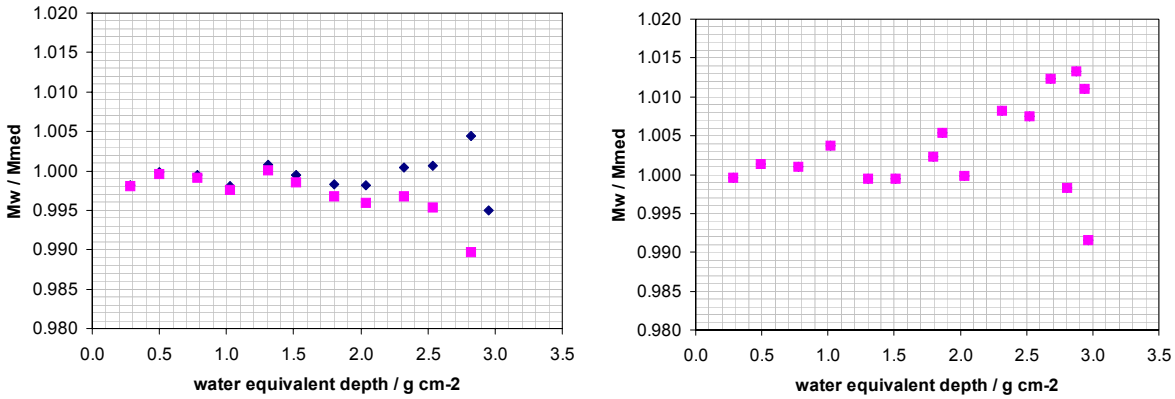

Resulting fluence correction for Al after correction for pristine (left) and full-modulated (right) beams:

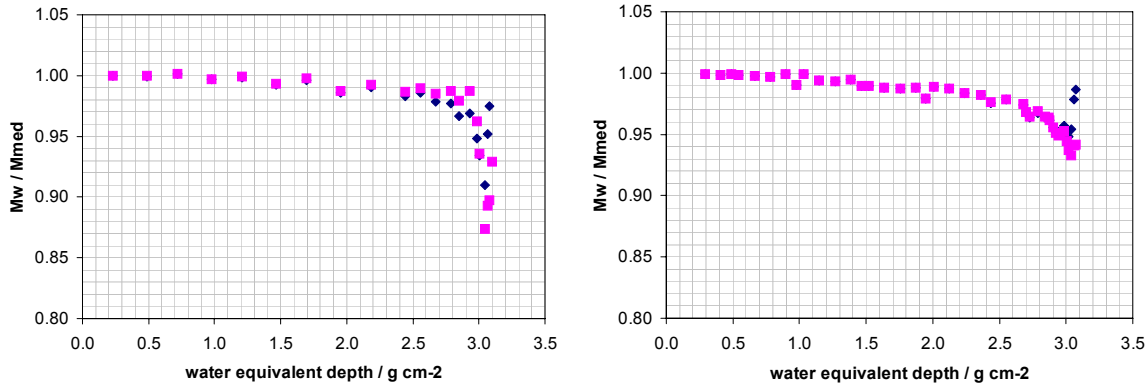

Resulting fluence correction for Cu after full-modulated beam:

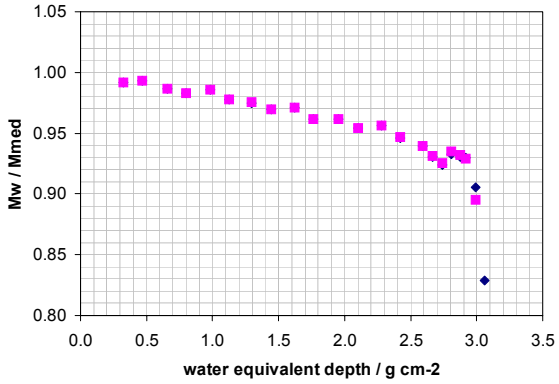

3. Analytical and Monte Carlo simulated fluence correction factors:

3.1. Analytical

Continuous slowing down approximation and local energy deposition of all energy transferred to charged particles for 60 MeV protons (left) and 200 MeV protons (right):

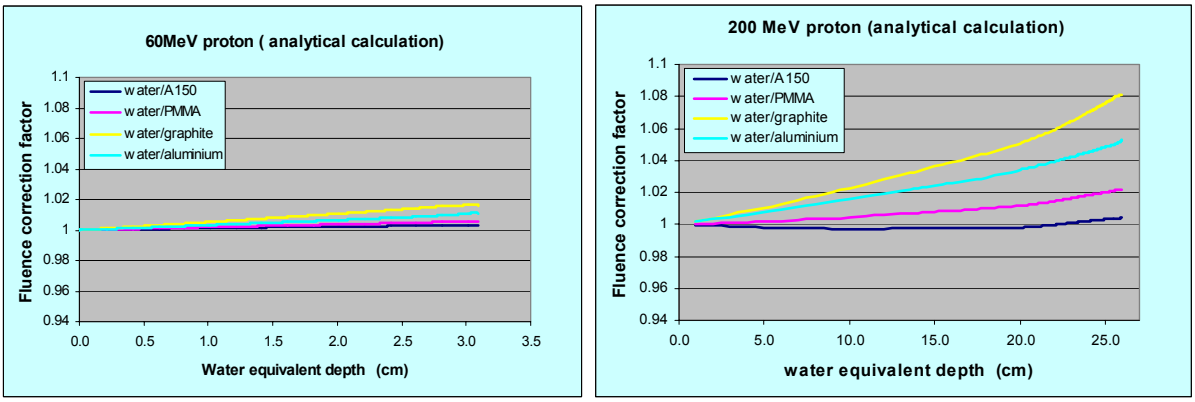

3.2. MCNPX

For 60 MeV protons (left) and 200 MeV protons (right):

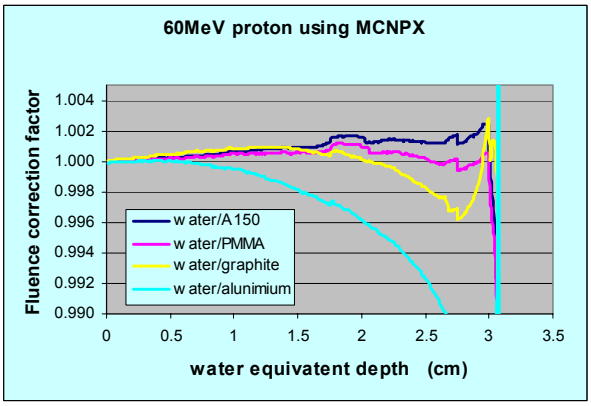

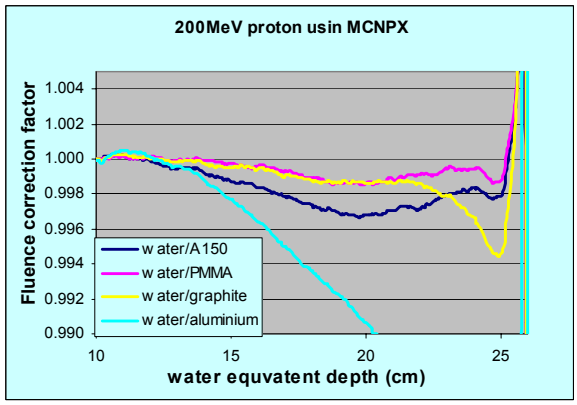

3.3. Geant4

For 60 MeV protons and only graphite to water conversion for CCO pristine beam (left) and for full modulated beam (right):
=

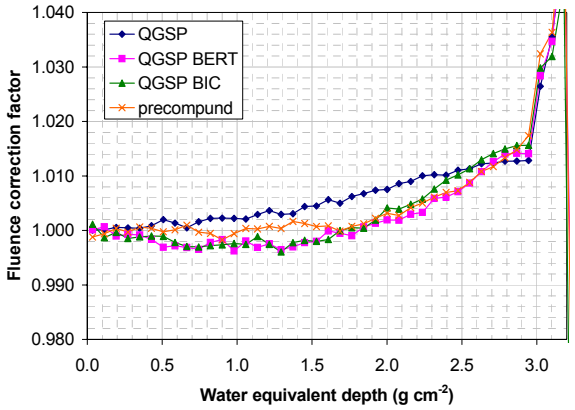

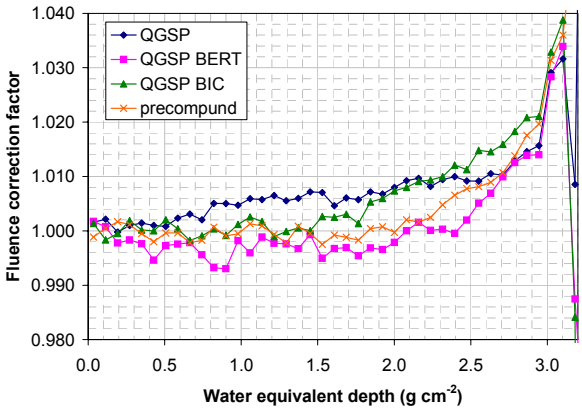

4. Attenuation measurements using large area Faraday cup

Measurements for water, graphite, PMMA, polystyrene, A150, aluminium, lead. Results for ranges within uncertainties in agreement with ICRU report 49 data.

Attenuation is a factor 2.5 larger than expected from ICRU report 63 total nonelastic cross sections.

Possible problem with experimental set-up found. To be investigated with MC simulations.

5. Ionization chambers

Comparative measurements were performed between NE2611, Markus, Roos and NACP02 chambers based on two calibration routes (reference to ^{60}Co and reference to 19 MeV electron beam).

Systematic deviations of 1% level between ion chambers with different wall materials were observed. It is complicated by disagreement in dosimetry according to the two routes.

Monte Carlo simulations of secondary electron perturbation suggest wall corrections up to 0.5%.

Analytical model based on secondary particle slowing down spectra suggest that perturbation due to different emission rates of alpha particles in oxygen and graphite could cause wall perturbations of level 0.5%.

2.3. B.V. Carlsson

Proposed work:

a) Calculation of proton-induced integrated, differential and double differential cross section and comparison with experimental data for a wide range of biological and structural elements, using exclusive a Double Differential Hybrid Monte Carlo Simulation (DDHMS) pre-equilibrium model (code to be developed and integrated into the EMPIRE system) coupled to Hauser-Feshbach or fragmentation equilibrium decay models (code for the latter must also be developed and integrated into the EMPIRE system).
b) Compare evaluated data files for proton-induced reactions (LA-150, JENDL, JEFF3.1 or ENDF/B-VII) with experimental data.

Progress:

a) An exclusive DDHMS module (XDDHMS) was developed but is still only partially integrated into the EMPIRE system. Residual populations are passed to the system so that equilibrium Hauser-Feshbach decay can be calculated. Differential and double-differential data accumulated in the calculation are converted from histogram to point data, for compatibility with the system, but are not yet passed correctly to the main program, so that complete spectra and double differential cross sections cannot be calculated.
b) The double-differential cross sections from XDDHMS calculations were compared with experimental data for proton-induced reactions on C, O, Al, Fe and Pb in the energy range from 14 MeV to 200 MeV. In general, the proton double-differential data are well described by the calculations at higher energies, although the cross section at backward angles tends to be underestimated. Discrepancies between the calculations and the proton double differential data increase as the energy decreases. The agreement of the calculations with neutron double differential data is at best only fair at high energies and also decreases as the energy is decreased. To try to improve these results, the algorithm for particle-hole energy selection will be modified to use a Fermi distribution rather than an equally spaced one and parameters will be tweaked.
c) ENDF-B/VII evaluated data files for proton-induced reactions were compared with experimental nonelastic reaction data for C, N, O, Ca, Fe and Pb. The evaluations extend up to 150 MeV. Their agreement with the experimental data was found to be quite good.
d) The rest of the proposed work was not completed, although work on the fragmentation module for the EMPIRE system has begun.

2.4. J.M. Quesada

Geant4 is a general purpose toolkit for the simulation of the passage of particles through matter [1]. Primary focus of Geant4 was on preparation of experiments for CERN Large Hadron Collider. Other areas of application are growing and include high energy, nuclear and accelerator physics, studies in hadronic therapy, tomography, space dosimetry, and others. Geant4 physics includes different models for simulation of interactions of hadrons with nuclei.

For the simulation of reactions of interest in hadrontherapy, the Bertini-style cascade (BERT) and the binary cascade (BIC) models are available. Both of them include, as final stages after the kinetic cascade regime, sequential pre-equilibrium and de-excitation phases.

Nevertheless, the high degree of accuracy required for practical applications needed for an overall improvement of the performance of the Geant4 hadronic models. In particular, our work has been concentrated in the pre-equilibrium and de-excitation models included in the binary cascade physics list. New physics has been included mainly through the implementation of more realistic inverse reaction cross sections for nucleons and light charged particles. An intensive bug-fixing effort has been made, which very much improved the description of charged particle emissions and fission. These achievements favoured the participation of Geant4 into the IAEA benchmark of spallation models [2]. Low energy region of the benchmark (below 200 MeV) and some materials of interest are common to hadrontherapy (structural materials for shielding, collimators, etc.), which justifies its inclusion in the present brief report.

For neutrons below 20 MeV, Geant4 High Precision parameterized model is recommended, although there is no direct access in Geant-4 to evaluated data in ENDF format; it uses some specific libraries which contain, in principle, the same type of information as the ENDF-6 format files, but they do not cover all presently evaluated nuclei and reactions. A coordination effort has been undertaken in this respect, fostering the collaboration with CIEMAT Nuclear Fission Department, which has developed a tool for generating these files from any presently existing evaluated data file [3]. As the main outcome of a recent meeting, it has been agreed to coordinate (JMQ and CIEMAT group) and make the additional efforts in order to make available those tools to qualified Geant4 users.

References

[1] S. Agostinelli, *et. al.*, Geant4 a simulation toolkit, Nucl. Instr. Meth. A506 (2003) 250.
[2] J. Apostalakis, A. Ivantchenko, V.N. Ivanchenko, M. Kossov, J.-M. Quesada, D.H. Wright, "Geant4 simulation of nuclear spallation reactions", Int. Topical Meeting on Nuclear Research Applications and Utilization of Accelerators, 4-8 May 2009, IAEA (Vienna, Austria).
[3] D. Cano-Ott, "Creation of new neutron transport Libraries for the Geant4 Code", private communication.

2.5. A. Ferrari

The CERN activities related to hadrontherapy in the period November 2007 - May 2009 can be summarized as follows. All these activities have been carried out in the framework of the development and application of the FLUKA code. FLUKA is a joint CERN-INFN project, and the code is widely applied to medical physics, in particular hadrontherapy problems. Most applications of the code in this field have been carried out at the Heavy Ion Therapy (HIT) centre in Germany by the researcher working in that facility.

Nuclear model development

The activities on nuclear models of some relevance for hadrontherapy carried out during the

period under consideration can be summarized as:

- Development of light ion interaction models according to the BME (Boltzmann Master Equation) approach below 100 MeV/n.
- Improvement of the Nucleon-Nucleus elastic and non-elastic interaction models.
- Development of a 260 group neutron transport library (0-20 MeV) based on the most recent evaluated nuclear data files.

Atomic Physics

Atomic physics is not a topic of interest for this working group, however it plays a major role in all hadrontherapy applications. Several development/studies have been carried out, concerning stopping power (refinement of higher order, Brach and Bloch, corrections, shell corrections for water, etc), and Compton interactions of photons with bound electrons (of relevance for PET or single photon detection).

Emitter predictions vs exp. data

Pioneering studies on PET online and offline for proton and heavy ion beams have been carried out with FLUKA at GSI, Boston (MGH), and Rossendorf. The analysis and comparison with simulations of the data taken at GSI with ^{12}C and ^{16}O beams in phantoms of several materials have been carried out at CERN in the framework of the PhD thesis of F. Sommerer. The results have been recently published (F. Sommerer et al., PMB54, 3979-3996, 2009).

HIT

FLUKA is used (mostly by K. Parodi and A. Mairani), at HIT, the first hospital-based Centre in Europe which will perform routine ion therapy, for several tasks. The code has been extensively validated against measured depth-dose distributions for protons and ^{12}C beams, and for ^{12}C beams, against available experimental data on fragment production and propagation in a water phantom, mostly at 400 MeV/n, making use of the preliminary data by D. Schardt *et al.*, as reported in the master thesis of E. Haettner. The wide range of applications of FLUKA code at HIT includes support to commissioning and quality assurance. The code has been used for the generation of the Treatment Planning System database. The generation of the HIT TPS basic data has been indeed performed with FLUKA. Dose profiles in water with and without ridge filter have been performed for all the 255 energies delivered by the accelerator for *p* and ^{12}C, as well as fragment spectra (for carbon ions only) for a grid of 37 equally spaced energies. FLUKA dose calculations of irradiated fields have been also extensively compared with measurements and TPS calculations to support the TPS-commissioning.

Questionnaire

An evolved draft of the questionnaire proposed at the previous RCM meeting has been prepared and submitted for discussion at this meeting. It is supposed to be finalized by the end of the meeting. Also, some research into existing experimental data which could have been of interest for benchmarking neutron production by proton beams on targets of relevance (biological and structural) has been carried out.

Sensitivity studies

An investigation has been carried out about the interplay of different physics processes for proton beams in water phantoms at energy, 200 MeV, relevant for therapy. In particular the role of nuclear interactions, multiple Coulomb scattering, and energy loss fluctuations on longitudinal dose profiles has been disentangled. Also the impact of different choices for the water average ionization potential ("I"), and of a possible initial beam momentum spread has been investigated.

Some sensitivity studies have been carried out as well for ^{12}C beams, at 270 MeV/n. The impact of variations (± 20%) in the reaction cross section on longitudinal dose and charged fragment distributions has been investigated. An algorithm has been developed in order to allow exploring variations in the angular distribution (transverse momentum in the centre-of-mass system) of particles and excited fragments after the interaction fast phase. The algorithm is designed such as to still correctly preserve conservation of basic quantities (energy, momentum, charge and mass). The impact of variations of ± 30% on the same longitudinal distributions has been investigated. Further impact of the model physics is being assessed (e.g. by changing the excitation energy of pre-fragments).

2.6. M.C. Morrone

The agreed work plan was the following:

a. Measurements of nuclear fragmentation of Carbon beams of 60-80 AMeV at INFN-LNS during 2008.
b. Specific agreement toward higher-energy measurements to be concluded in 2008
c. Measurements of nuclear fragmentation in carbon beams up to 400AMeV to be undertaken in 2009-2010 depending on the beams availability

We measured the fragmentation of ^{12}C beam accelerated by the Superconducting Cyclotron at 32 AMeV and 62 AMeV on ^{197}Au, ^{207}Pb and ^{12}C targets at the INFN Laboratori Nazionali del Sud in Catania. During those measurements we did not have the possibility to measure the number of primaries. For this reason the reported cross sections have been normalized using elastic scattering data.

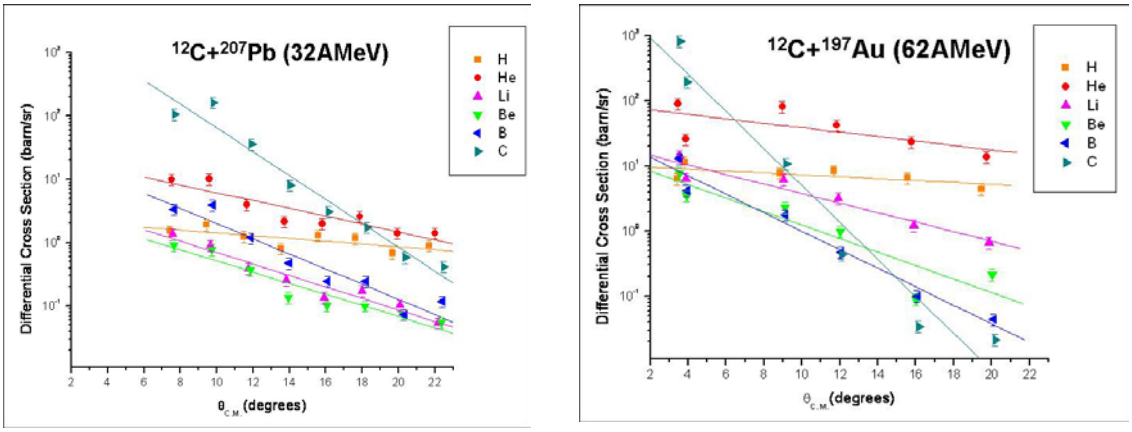

Fig. 1: Fragmentation of the incident carbon beam on lead and gold

Fig. 1 shows the measured angular distribution of the reaction products for ^{12}C + ^{197}Au at 62 AMeV and ^{12}C + ^{207}Pb at 32 AMeV. We observe that the obtained angular distributions are similar in both cases and fragments, at the highest incident energy, are emitted at forward angles. Moreover the angular distribution of light fragments such as protons and alpha particles is more isotropic than the one corresponding to heavier fragments due to different production mechanisms. In Fig. 2 we report a comparison between the absolute cross sections for the two considered systems in the angular range ±3°÷± 20°. This comparison shows that the main contribution to fragments cross section is due to alpha particles, as it is expected from the ^{12}C "cluster α" assembly, and that doubling the energy causes fragments cross-section a factor ten higher, *suggesting an energy dependence in the fragment production mechanism*.

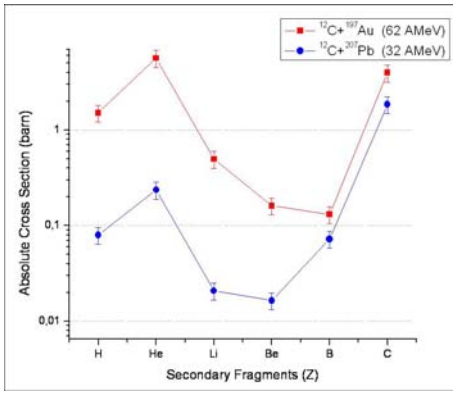

Fig 2: Absolute cross sections the reaction products for ^{12}C + ^{197}Au at 62 AMeV and ^{12}C + ^{207}Pb at 32 AMeV.

A second run, with high statistics and adding a Faraday cup on the beam line to measure the beam current, has been performed during April 2009, using a ^{12}C beam of 62AMeV. Tree targets were used: C, Au, CH_2. The data analysis is in progress. A request for further beam time to perform fragmentation measurements at 80AMeV in autumn 2009 has been submitted to the LNS PAC and the answer is expected by the end of July 2009.

Theoretical double differential cross sections for proton and alpha particles computed with two different Hadronic physic models, Binary light ion cascade (BIC) and Quantum Molecular Dynamic (QMD) differ by an order of magnitude (Fig.3).

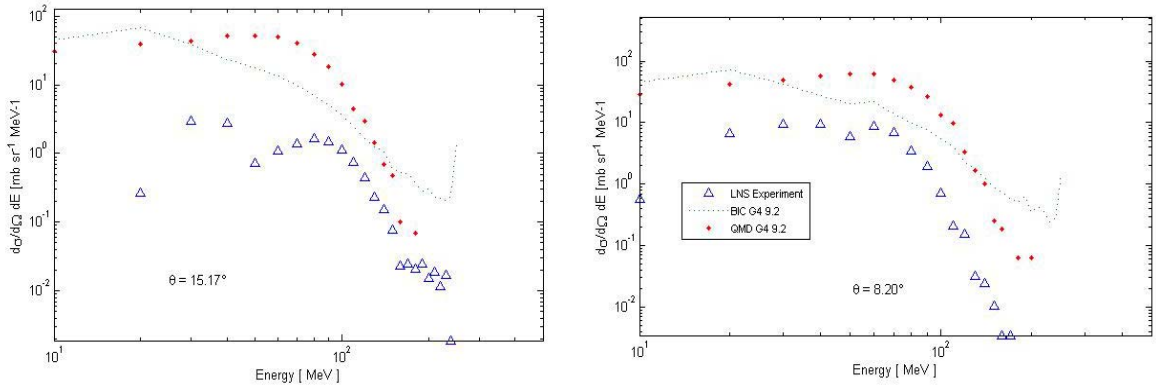

Fig. 3: Experimental data ^{12}C + ^{197}Au at 62 AMeV vs. Geant4 (based on BIC and QMD Hadronic Models)

Report on item 2

In 2008 INFN defined a collaboration with GSI and CEA Saclay related to a campaign of measurements to be carried out up to 400 AMeV based on the use of Aladin+Music+TOF+Land+Catania Hodoscope at GSI. The first result of this collaboration has been the definition of a proposal at GSI-GPac presented at the end of February and approved for 33 BTU to be undertaken at the end of 2010.

Report on item 3

The GSI experiment has been approved, based on the specific detectors Aladin+Music+TOF +LAND+Catania hodoscope. The interest for differential cross section measurements of high energy projectile on thin targets is due to the fact that the primary ions fragmentation cannot be experimentally measured in any real condition for hadrontherapy applications. Only by measuring those cross sections, we can have suitable perspectives to develop and validate nuclear interaction models to be implemented in MC codes.

The characterization of the fragmentation decay allows simultaneously a variety of physics cases: from the measurements of the double differential fragmentation cross-section to a study of the mechanism itself. Processes differ as a function of energy: production mechanisms go from transfer reactions, observed at low energies, to "pure" fragmentations processes observed at the highest energies, around 1 AGeV. At high energy according to a phenomenological point of view, fragments are produced with a velocity slightly lower than that of the beam and are emitted in a rather small cone around the direction of the incident beam. Thus the experimental apparatus that had to detect projectile fragments should only cover the forward angles with respect to the beam direction. Among the detector scenario which could be suited for such experiment, namely the FRS setup and the Aladin setup we foreseen the latter since, for light projectile, fragmentation due to the momentum (1%) and angular ($\Delta\Theta_{x,y}$ = ±13mrad) acceptances, the FRS setup could put serious limitation on the determination of the cross-sections.

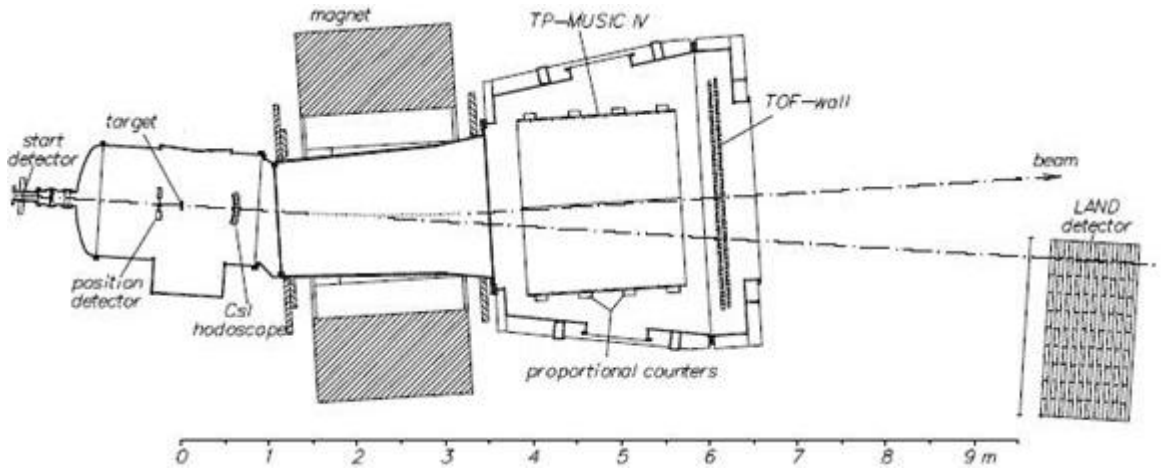

Fig. 4: Cross sectional view of the Aladin setup.

A cross sectional view of the setup is shown in Fig. 4. The beam enters from the left and passes thin time- and position-detectors before reaching the interaction target. Projectile fragments entering into the acceptance of the magnet are tracked and identified in the TP-MUSIC IV detector and in the time-of-flight (TOF) wall. Neutrons emitted in directions close to $\theta_{lab} = 0^{\circ}$, are detected with the Large-Area Neutron Detector (LAND). The dash-dotted lines represent the beam directions before and after the deflection by 7° in the field of the Aladin magnet. The measurement of the charge and the momentum vector of all projectile fragments with $Z \geq 1$ will be performed with high efficiency and high resolution with the

TPMUSIC IV detector. In order to cover the wide dynamic range necessary to measure nuclei over a wide charge range with the best possible resolution, two different kinds of detectors are connected to the field cage of the TP-MUSIC detector on either side: the ionization charge collected at 24 anodes provides optimum Z resolution for heavy fragments (Z>8), whereas the 3D tracking information of all particles and the charges of lighter fragments are obtained from 4 position-sensitive proportional counters. The position of the ionizing particles in the non-bending plane is determined from the position along the proportional counters, whereas the position in the bending plane is determined by measuring the total drift time of the electrons to the detectors.

The proportional counters use a combination of charge-division and pad-readout techniques to reconstruct the position in the non-bending plane of the tracks of nuclei. The pads of each section are connected modulo five: the resulting position ambiguity can indeed be resolved by using the less precise position information obtained from the anode wires with the charge-division method.
To extract the signals from each sector of the proportional counters, seven charge-sensitive preamplifiers are used. The signals of the preamplifiers, after removal of the high frequency component through an anti-aliasing filter, are digitized by 14-bit Flash ADC's without prior shaping. The typical noise is of 1 Least Significant Bit (standard deviation) over a dynamic range of $1 : 10^4$. The output, generated at a rate of up to 40 MHz, is stored and processed by a system containing FPGA and *DSP chips.*

On the same board fast-digital and high-resolution analog circuits are operating without deterioration of the resolution. Such a detection system, with its dedicated electronics, is providing at the same time high resolution, a large dynamic range and multi-hit capability. Using the reconstructed values for the rigidity and path length, the charge of the particle measured by the TP-MUSIC detector, and the time of flight given by the TOF-wall, the velocity and the momentum vector can be calculated for each detected charged particle.

The knowledge of velocity and momentum allows then the calculation of the particle's mass. Single mass resolution for charges up to 12 is obtained, corresponding to a mass resolution $\Delta A/A$ of approximately 4.0% (FWHM) for light fragments. We are going to upgrade the Aladin+Music+TOF +LAND+Catania Hodoscope setup in the interaction region. The main goal of the upgrades is to achieve the needed time and momentum resolution even in the case of the light beam (C and O) setup. Following the beam path the improved setup will have a TOF start counter, a beam tracker chamber, the target and a "vertex" detector. The insertion of two tracking devices has the aim to have a precise information of the beam impact point in the target and to have a first measurement of the produced fragment tracks nearby the target, before the Aladin magnet. This information should help the several meters backtracking of the fragments from the MUSIC through the magnetic field, as well as the fragment emission angle determination at the target.

Such a design is particularly useful for light beams, where the start counter must have enough thickness to achieve a resolution for the TOF system of the order of 400 ps (including the TOF wall contribution). In this case the beam track chamber can detect (and veto) secondary product of eventual interaction of the beam in the start counter. Common design issues for both detectors are the reduced size, the low material budget (interaction probability at the % level), good spatial hit resolution (order of 200 μm) and operation in vacuum. Furthermore the vertex detector must also have good track separation capability. Given these constraints we are evaluating several solutions, among which a drift chamber for the beam detector and a very thin silicon detector for the vertex detector. The Catania Hodoscope, an array of 96 two

fold telescope (300 μm Si followed by 6 cm long CsI with photodiode readout), already used by the Aladin collaboration in a number of different experiments, will be placed at the entrance of the Aladin magnet surrounding its hole. This will allow recovering those light particles from the decay which do not enter the acceptance of the magnet.

2.7. K. Niita

Summary of undertaken activities:

(a) Review of the cross-section data for the simulation of the radiotherapy applications. As for the secondary particle production by heavy ion collisions, we have picked up the following published data.

1) "Handbook on Secondary Particle Production and Transport by High-Energy Heavy Ions" by T. Nakamura and L. Heibronn.
2) "Overview of secondary neutron production relevant to shielding in space", L. Heilbronn, et. al., Radiation Protection Dosimetry 116, (2005) 140.
3) "Cross sections for the production of residual nuclides by high-energy heavy ions", H. Yashima, et.al. Nucl. Instr. and Meth. B226, (2004) 243.
4) "Influence of fragment reaction of relativistic heavy charged particles on heavy-ion radiotherapy", N. Matsufuji, et.al., Phys. Med. Biol. 48, (2003) 1605, and "Spatial fragment distribution from a therapeutic pencil-like carbon beam in water", Phys. Med. Biol. 50, (2005) 3393.
5) "Measurements of total and partial charge-changing cross sections for 200- to 400-MeV/nucleon 12C on water and polycarbonate", T. Toshio, et. al., Phys. Rev. C75 (2007) 054606.
6) "Experimental fragmentation studies with 12C therapy beams", E. Haettner, et.al., Radiation Protection Dosimetry 122, (2006) 485.
7) Secondary beam fragments produced by 200 MeV u-1/2 12C ions in water and their dose contributions in carbon ion radiotherapy", K. Gunzert-Max et.al, New Journ. of Phys. 10, (2008) 075003.

(b) Sensitivity study of the cross-section data implemented in the PHITS code.

1) Sensitivity study for the charged particle energy losses in water
We have reviewed the SPAR code and ATIMA package (*Nucl. Instr. Meth.* 114, **B136**, 1998) and checked the sensitivity on the ionization processes by these codes.
2) Sensitivity study for the total reaction cross sections of heavy ion collisions
We have analyzed the sensitivity on the dose distribution by changing the total reaction cross sections for heavy ion collisions. For this, we used two cross section parameterizations employed in the PHITS code.
2.1.) Shen formula: Nucl. Phys., 130, **A491,** 1989
2.2.) NASA systematics: Nucl. Instr. and Meth. 349, **B155,** 1999.
3) Sensitivity study for the total and elastic cross section of proton induced reactions
We have analyzed the sensitivity on the dose distribution by changing the total reaction cross sections and elastic cross sections for proton induced reactions. The basic parameterization of these cross sections used in the PHITS code is referred in Nucl. Instr. and Meth. 406, **B184**, 2001

(c) Reference settings for the radiotherapy applications in the PHITS code.

1) Sensitivity study for the detailed parameters used in the PHITS code
   We have checked the dependence of the parameter, the switching time, in the PHITS code on the depth dose distribution of carbon beam.
2) reference settings
   We have proposed the reference settings of the PHITS calculation for radiotherapy applications.

2.8. N.M. Sobolevsky

(presented by O Jäkel and A Botvina)

Collection and compilation of experimental data related to particle therapy.

Files were collected with experimental data on particle and fragment production in reaction initiated by protons and carbon ions. The projectile energy range was selected to be corresponding to the energies important for particle therapy. In particular, Ep = 50 - 800 MeV for proton beams, and E_C = 10 - 400 MeV per nucleon for carbon beams. As targets, elements of H, C, N, O, F, Na, Mg, P, S, Cl, K, Ca, typical for biological tissue, were adopted.

The data involve:

- total reaction cross sections (in mb)
- Double differential cross sections of secondary particle production (as neutrons, protons, alpha-particles, fragments).
- Cross sections of radionuclide production, such as PET isotopes (e.g., ^{11}C and ^{15}O).

New calculations carried out with SHIELD-HIT have demonstrated that experimental data can be well reproduced with this code. We have found also that an intercomparison between different models is very promising, and it can explain the influence of special model parameters. The most promising results are related to the distribution of produced PET isotopes. It is shown that these isotopes are concentrated around the Bragg peak region.

Another promising development is to use direct photons, produced after decay of excited levels of isotopes, for monitoring purposes. The Fermi-break-up model implemented into SHIELD-HIT gives a possibility for extensive calculation of this effect.

2.9. A. Heikinnen

A report of the Geant4 activities undertaken in 2008 and early 2009 related to the project has been presented. Several members from Geant4 collaboration have participated in the CRP. We have prepared an open source Geant4 code, to allow its use by non Geant4 members. This open source code acts as a platform for benchmarking and other tasks to be made in the CRP. The code is based on Geant4 Hadrontherapy example prepared by INFN-Catania collaborators and test30 which is originally used for internal validation of Geant4 hadronic models.

3. Benchmarks

1. E. Haettner data (200 AMeV and 400 AMeV); one issue is the availability of the data: OJ+AH coordinate obtaining and distributing the data within this group. The numerical data are needed for a real benchmark.
   - Agreement from Dieter to use the data (OJ then RC then AF+AH+…)
   - Request clear description of the data and experimental conditions for a benchmark

   Note: Yields are published in Radiation Protection Dosimetry journal. Spectral and angular distributions are available only in thesis.

2. C. Morrone data (62 AMeV): make sure all required info for benchmark is recorded.

3. One or two thick target neutron production data; see section 3.5 – all codes involved.

4. Thin target proton emission spectra; 2 energies (between 100 MeV and 200 MeV) for which there are sufficient angle integrated data. Targets C, Fe and high-Z

5. MLCF for protons; done for SHIELD, Geant4 and FLUKA. PHITS will also participate. MCNPX: ICCR 2000 paper Heidelberg. Numerical data (64 numbers), geometry (64 thicknesses) and beam data (energy and energy spread) available from HP -> provide to RC.

6. Kerma comparison for ion chamber dosimetry (just comparison of codes with evaluated data).

Others?

7. Toshito Phys Rev C75:054606 and Toshito Phys Rev C78:067602 data on charge-change cross sections? Compare cross sections for first paper.

8. Alanine experiment in carbon ion beam (Rochus Hermann < data OJ) and proton beam (NPL < HP).

Actions:
RC will organize and track progress with the benchmarking exercises, including periodic telephone conference calls.

4. Project Web Site

The CHARPAR project area has been set up on the NDS server running under Linux operating system for exchanging information. It is accessible as http://www-nds.iaea.org/charpar/

5. Conclusions

Presentations and discussions during the meeting showed that there is a consensus regarding

the tasks required to achieve the planned goals of the CRP. The programme to compile and evaluate charged-particle nuclear data for therapeutic applications was reviewed. Furthermore, by discussing the various issues related to nuclear data, detailed planning of both remaining tasks in general and for each member of the group was accomplished. Issues related to data collection and compilation, sensitivity studies, benchmarks and dosimetry for proton as well as heavy-ion radiotherapy were extensively debated. Further extensive work needs to be done in the next 15 months so that the necessary progress can be achieved before the final RCM.

It was recommended to hold the next Research Coordination Meeting in Summer 2010 either in Heidelberg, Germany or Vienna, Austria.

Appendix 1: Agenda

2nd Research Coordination Meeting on

"Heavy charged-particle interaction data for radiotherapy"

National Institute of Nuclear Physics (INFN)
Catania, Italy
8 – 12 June 2009

MONDAY, 8 JUNE

08:30	***Pick-up at Katane Palace Hotel*** **(**Via C. Finocchiaro Aprile n° 110) for collective transfer to meeting premises at INFN-LNS[3]
	Discussion of organizational aspects
09:30 - 10:00	**Opening Session**
	Welcoming address – Giacomo Cuttone (INFN)
	Introductory Remarks – Roberto Capote Noy (IAEA)
	Election of Chairman and Rapporteur
	Adoption of Agenda
10:00 - 12:30	**Presentations and status reports**
	(Please provide a one-page written summary of undertaken activities for each contract/agreement within the CRP)
12:30 – 14:00	***Lunch***
14:00 – 18:00	**Presentations and status reports (cont.)**
	Coffee break as needed

TUESDAY, 9 JUNE

08:30	***Pick-up at Katane Palace Hotel***
09:00 - 12:30	**Presentations and status reports (cont.)**
12:30 - 14:00	**Lunch**
14:00 – 18:00	**Discussions on key topics:**
	Treatment head simulations and beam characteristics.
	Coffee break as needed

WEDNESDAY, 10 June

08:30	***Pick-up at Katane Palace Hotel***
09:00 - 12:30	**Discussions on key topics (cont.):**
	Primary standards and reference dosimetry.
	Activation for PET.
12:30 - 14:00	**Lunch**
14:00 – 18:00	**Discussions on key topics (cont.):**
	Neutron production for protection.
	Treatment planning dose calculations.
	Coffee break as needed
	DINNER (courtesy of INFN)

[3] Transport back to the Katane Palace Hotel will also be provided each day of the meeting after conclusion of sessions.

THURSDAY, 11 JUNE

08:30	***Pick-up at Katane Palace Hotel***
09:00 - 12:30	**Summary of the work to be done for the next 18 months** All topics
12:30 - 14:00	**Lunch**
14:00 – 18:00	**Drafting of the Summary Report of the Meeting**

Coffee break as needed

FRIDAY, 12 JUNE

08:30	***Pick-up at Katane Palace Hotel***
09:00 - 12:30	**Review and Approval of the Summary Report**
12:30 - 14:00	**Lunch**
14:00 – 15:00	**Closing of the Meeting**

Coffee break as needed

Appendix 2: List of Participants

2nd Research Coordination Meeting on
"Heavy charged-particle interaction data for radiotherapy"
National Institute of Nuclear Physics (INFN)
Catania, Italy
8 to 12 June 2009

BRAZIL

Brett Vern Carlson
Instituto Tecnologico de Aeronautica (ITA)
Praça Mal. Eduardo Gomes, 50
Vila das Acácias
12228-900 Sao Jose dos Campos, SP
Tel: +55 12-3947-6881
Fax: +55 12-3947-5050
E-mail: brett@ita.br

FINLAND

Aatos Heikkinen
Helsinki Institute of Physics
University of Helsinki
P.O. Box 64
00014 Helsinki
Tel: +35 891 9150560
Fax: +35 891 9150522
E-mail: aatos.heikkinen@gmail.com
aatos.heikkinen@cern.ch

GERMANY

Oliver Jäkel
Deutsches Krebsforschungszentrum (DKFZ)
Deptm. of Medical Physics in Radiation Oncology (E040)
Im Neuenheimer Feld 280
69120 Heidelberg
Tel: +49 6221 422596
Fax:
E-mail: o.jaekel@dkfz-heidelberg.de

JAPAN

Koji Niita
Research Organization for Information Science & Technology
Tokai-mura, Naka-gun
Ibaraki-ken 319-1106
Tel: +81 29 282 5017
Fax: +81 29 287 0315
E-mail: niita@tokai.rist.or.jp

SPAIN

Jose Manuel Quesada
Facultad de Fisica, Universidad de Sevilla
Av. Reina Mercedes S/N
Apartado de Correos 1065
41080 Sevilla
Tel: +34 954486469
Fax: +
E-mail: quesada@us.es

UNITED KINGDOM

Hugo Palmans
National Physical Laboratory (NPL)
Acoustics and Ionising Radiation Team
Hampton Road
Teddington TW11 0LW
Middlesex
United Kingdom
Tel: +44 20 89436568
Fax: +44 20 99436070
E-mail: hugo.palmans@npl.co.uk

ITALY

Maria Cristina Morone
Dept. of Biopathology and Diagnostic Imaging
Division of Medical Physics
University of Rome Tor Vergata
Via Montpellier No. 1
00133 Rome
Tel: +39 06 7259 60 17
Fax: +39 06 7259 63 89
E-mail: cristina.morone@roma2.infn.it

INTERNATIONAL ORGANIZATION

Alfredo Ferrari
European Organization for
Nuclear Research (CERN)
1211 Geneva 23
Switzerland
Tel: +41 22 76 76119
Fax: +41 22 76 69474
E-mail: alfredo.ferrari@cern.ch

CONSULTANT

Alexander Botvina
Institute of Nuclear Research
Russian Academy of Sciences
Profsojuznaya 7A
117312 Moscow
Russian Federation
Tel. +
Fax +
E-mail: a.botvina@gsi.de

UNITED STATES OF AMERICA

Harald Paganetti
Massachusetts General Hospital
Department of Radiation Oncology
FHB Proton Therapy Center
Fruit Street,
Boston, MA 02114
Tel: +1 617 726 5847
Fax: +1 617 724 0368
E-mail: hpaganetti@partners.org

OBSERVER

Katrin Henkner
German Cancer Research Center (DKFZ)
Dept. of Medical Physics in Radiation
Oncology
Im Neuenheimer Feld 280
69120 Heidelberg
Germany
Tel: +49 6221 42 2416
Fax: +
E-mail: k.henkner@dkfz-heidelberg.de

IAEA

Roberto Capote Noy
Nuclear Data Section
Division of Physical and Chemical
Sciences
Wagramer Strasse 5
1400 Vienna
Tel. +43-1-2600 21713
Fax +43-1-2600 7
E-mail: r.capotenoy@iaea.org

Appendix 3: Per Topic – What We Know. Where We Have to Go.

General

Collection of experimental data on nuclear reactions in the context of hadron therapy

New / achieved	To Do
*Interaction data: - Compilation by N. Sobolevsky: comprehensive (AF: what are we going to do with these data) - GSI data - IAEA: experimental elastic data for C, Fe, W + optical model data above 200 MeV - Published Japanese data on charge-change cross sections: Toshito Phys Rev C75:054606 + Toshito Phys Rev C78;067602 - Brett's data for protons / most elements up to 150 MeV (total nonelastic, neutron differential) - dd experimental data INFN	* Interaction data - Review Elastic data for N (?), O (and optical model) : RC+BC - Nonelastic data for N, O and materials identified: RC+BC (thin target data) + which one can be used for benchmarking RC: update list of Nikolaj with refs AF: Check completeness of data, check ref Carlson 1996. -> to be continued: CM: Fragmentation data 62 AMeV carbon ions on C, Au, CH2 80 AMeV experiments by the end of 2009 -> AF to provide
* Needs: neutron d-d data thick target Charged particle prod: angular integrated LANL 114 MeV: Nucl Sci Engin 102:310 (1989) LANL 256 MeV: Nucl Sci Engin 110:289 (or 299) (1992) 68 MeV Jap Rep; Be, C, Al, Au	Compilation of all these references: - For protons (C, Fe, high-Z targets): Thick target data -> AF Thin target data -> RC (lanl & xfor) - For ions? (Fragmentation data is more important, nuclear elastic is assumed to be negligible, but proven?). Maybe one case; C on C thick target neutron prod; 135, 290, 400 AMeV (publication X<Niita) ->data in EXFOR
* Identify materials For protons and ions: done for treatment head, patients and dosimetry. Review ridge filters materials (Al, PMMA)	* Identify materials --

Questionnaire

New / achieved	To Do
First draft Define recipients: geant4 (Aatos will organize developers+some power-users for appl), MCNP (Mark+Goorley), FLUKA (Alfredo), PHITS (Koji), SHIELD (Nikolaj), VMCpro (Soukup), PETRA (Medin), HIBRAC (Sihver), SRNA (Ilic), PRONTO (Traneus)	Deadline for comments from this group: 1 month after the meeting: Other codes? Contact people at conference if need SRNA RC to contact MCNP people Varian, IBA/CMS (carbon bt also proton) ? GC will ask Hana Kafruni about Nucletron Need to make distribution list

Treatment Head Simulation and Beam Characterisation

Protons

New / achieved	To Do
Sensitivity analysis: Simulations showing importance of secondaries in phsp for scattered beam (even less for scanned) For absolute Monitor calibration contribution from secondaries quantified (1%) Energy distibutions of neutrons from treatement head Contribution to primary proton fluence quantified - impact of realistic uncertainties on xsections is small (50% error would only give 1% error on dose) Review of data:	 No additional information needed No additional data needed for secondary protons Angular distributions for neutron fluence from treatment head. Look at sensitivity to angular distributions from brass (p,n on Zn and Cu) (thick target) Could be combined with runs for other simulations Pencil beam on brass. Te be specified: beam energy, thickness of target, threshold, distance from target of scoring plane, what is scored (leakage from target) Geant4: HP FLUKA: AF PHITS: KN MCNPX(?) No further work needed

Phsp too complex for scattered beams; one paper by Paganetti. For scanned beams it is trivial Data and parametrisations: See under questionnaire	

Ions

New / achieved	To Do
Sensitivity analysis Not done on metal. KN some people have done simulations Neutrons not important; few outside of field, behind BP high-energy (published information shows less neutrons at carbon facilities than protons Med Phys 35:4782 (2008))	KN to simulate a simple case (pencil beam) and estimate sensitivity for neutron emission from proton and carbon What about influence ridge filter on primary beam. Probably spectra not very different (RBE is same within uncertainties for scanned and passive beam). GC: Main contribution is 4He; simulation done of 4He contrib -> extract info. Koji check data from Matsufuji; A simulation could be done -> GC, OJ (confirmation that there is not a large difference)

Primary Standards and Reference Dosimetry

Protons:

New / achieved	To Do
Sensitivity: - Calorimetry: Experimental graphite to water dose conversion in low-E protons + simulations in high-energy. Experimental other materials to water dose conversion in low-E protons + simulations in high-energy. Only total reaction cross sections required + angle integrated emission spectra (secondary protons)	-> elastic scattering? AF: angular distributions, 2 energies, oxygen (200 MeV, 65 MeV) and carbon (200 or 185 MeV, 65 MeV) + H-H (almost isotropic) RC can also provide data for carbon (see above)

- Ionization chambers Total reaction cross sections required + angle integrated emission spectra (secondary protons + alphas) List of materials: C, O, water, aluminium, PMMA, polystyrene, water plastics, A150, Fe	-> MC simulation of nonelastic interaction perturbation for IC needed (p_Q in k_{Q,Q_o} expression); determine sensitivity -> HuP+DavidShipley AF: ratios of production channels (partial kermas), maybe not at 20% level e.g. difference N and C (+importance of short range secondary particles) Three excercises: - compute partial kermas (AF, KN) + compare with evaluated data - idealized ion chamber simulation (air cavity in water + graphite wall) -> David Shipley? - monitor chamber simulation for carbon ions (HP) Simulation of the Faraday cup attenuation experiment

Ions

New / achieved	**To Do**
Calorimetry Ion chambers: Effect of projectile fragments has been looked into; small	Graphite to water dose conversion? - Experiment may not happen within next year. Will check opportunity. (OJ+HuP) - Simulations; depends on availability of student (OJ) -> effect of short range target fragments (e.g. aluminium central electrode & those produced in the gas) that enter ion chamber should be investigated HP: possible simulation of monitor IC for C-ions with geant4 (track length) (pencil beam in large area IC -> reciprocity) GC: for ion chamber simulations codes are not at level of e.g. Penelope, egsnrc for elecrons The same exercise on ion chambers for carbon ions as for protons (OJ+)

Activation for PET

Nuclear data for charged-particle therapy monitoring with PET

New / achieved	**To Do**
Protons: INDC(NDS)-0535: summary report on high precision beta+ emitters; most important radioisotopes. Well known for ions, for protons many more isotopes/half lifes, etc Best available data: http://www-nds.iaea.org/medical/positron_emitters.html	
Ions: AF: Calculated 11C and 15O production data, model based, for carbon ion beams in phantom have been published (water, PMMA, graphite phantom). Is it of practical use for other codes? -> pure comparison of simulations sufficient? No modeling of detection system.	For ions there is a lack of basic data. Not much can be done. HIT will not have online PET. Will have offline PET. Recommendation on which data are needed depending if you do on-line or off-line PET? For off-line: 2 isotopes (11C and 15O). For in-beam: for proton and C-ions to be collected -> RC. Maybe 10 or more for ions (incl projectile fragmentation); [Monte Carlo work package 6 in Envision (FP7): MC for production beta emitters for carbon therapy; geant4 or fluka -> RC to provide slide with group, scope to GC for presentation] Simulations with SHIELD-HIT < NS, FLUKA <Katia Parodi. Rossendorf may install in-beam PET <OJ

Prompt gamma imaging? Combine this with sub-section on PET.

New / achieved	To Do
Protons: Experiments Korea, MGH (demo it is measurable) Monte Carlo simulations MD Anderson, MGH AF: for low-E data available but not convinced there are so much data. Ions: Exploratory work just started. Probably a lot of gaps for ions	Question is if we want to cover this or just restrict to comment (revisit within next year). For carbon ions 11B maybe more correlated to Bragg peak position. HP summarise what is out there by next meeting

Neutron Production for Protection

New / achieved	To Do
Defined which data we have to test against. d-d data icru in disagreement with experimental data (at large angles; is it relevant?) sensitivity analysis on neutron energy distributions done (MGH) fluence, not dose. Disagreement geant4-mcnpx; mcnp probably more reliable regarding propagation of neutrons.	Benchmarks of thick target data. Data are there (not thermal). In case problems with thick targets it could be useful to consider also thin targets; but it should not drag us to nuclear data benchmarking exercise. Calculation of neutron energy spectra with all codes (HP, AF, KN, NS,…+ someone MCNPX). But it is unclear what differences mean. 256 MeV (<LANL) and 68 MeV (< JM); thick target; C, Fe, Pb (or other high-Z); AF will provide numerical data We can simulate dose, but what is relevant is RBE, For protection: use ICRP conversions to evaluate; for

	patient? Suggest to use same approach; we do not want to go in this deeper. Simple fluence to dose conversion to evaluate how sensitive it is
Shielding Materials: Carbon, Fe, heavy (depending availability) see above Experiments done in MGH. Compared with geant4 (for the MatriXX detector). But probably not doable for other codes; unless e.g. bonner sphere models are already in code. Maybe also not needed.	Shielding Regarding shielding; if we get results of exercise, evaluate effect if substantial -> we can still decide to go deeper covered by thick target excercise

Treatment Planning Dose Calculations

Protons:

New / achieved	To Do
Enough data on secondary protons. 30 plans: good statistics Dose to tissue to dose to water conversion covered. Sensitivity evaluated for these applications. Contribution is 2-5% of target dose. Have to be taken into account but requirements on nuclear data not so stringent (clinically not significant). SHIELD-HIT simulation of MLCF results	A comparison between MGH (geant4) and MD Anderson (MCNPX) will be performed for patient dose calculations. Has to be evaluated if secondary contributions can be separated. Planned geant4 simulations of PSI beams and frame experiment (see previous report). HP: clarify with Tony how to progress.

Carbon Ions

New / achieved	To Do
Rely on measured fragmentation data from GSI (thick target). We know it is more important for carbon ions than for protons. Sensitivity evaluated for absorbed dose but more complicated for RBE.	Dose calculation on one or two patient cases. Evaluate contributions of different fragments. Dose distributions and LET distributions. More than one code? Compare FLUKA-YIELD. Possibly also geant4 (INFN), PHITS and SHIELD-HIT (?->KH and NS) but problem is exchange DICOM and material data. Patient or simpler phantom? Water phantom -> no issue with the patient, dicom data etc, but you can only calculate dose and LET (OK for projectile fragmentation less for secondary effect of target fragmentation). -> Decided for water phantom
SHIELD-HIT simulation of MLCF results. Probably not useful as benchmarking tool since it cannot distinguish between reaction channels Experimental PDDs behind different materials (cortical bone, adipose) not sensitive to fragmentation cross sections.	-> KH further investigate if there is some sensitivity to fragmentation channels

Nuclear Data Section
International Atomic Energy Agency
P.O. Box 100
A-1400 Vienna
Austria

e-mail: services@iaeand.iaea.org
fax: (43-1) 26007
telephone: (43-1) 2600-21710
Web: http://www-nds.iaea.org